3 8006 10058 4989

CoA Memo. No. 192

Vibrations of the Propeller Shaft and the Rear Axle of a Passenger Car

- A progress report -

By: A.K.Egbuson
D.Hodgetts
& R.Hodgson

COLLEGE OF AERONAUTICS LIBRARY

Summary

Digital analysis of the free-free bending vibrations of a propeller shaft and a beam-type rear axle are compared, for different theoretical models, with the results of rig tests. The relative importance of distributed mass, the coupling between the bending and torsional modes and the half shafts of the rear axle are discussed. The relation between the work completed and the programme of work in progress is given briefly at the end of the report.

Nomenclature

a	$\sqrt[4]{\frac{\mu\omega^2}{EI}}$ per inch
E	Young's Modulus, lbf/in^2
f_o	Fundamental frequency, cycles/sec.
f_n	nth order natural frequency, cycles/sec.
G	Modulus of rigidity, lbf/in^2
I	Area moment of inertia, in^4
I_p	Polar second area moment, in^4
$I_{\alpha B}$	Mass moment of inertia of mass B about an axis perpendicular to the plane of bending, and passing through the centre of gravity of B, lbf.sec^2.in.
J	Moment of rotational inertia, lbf.sec^2.in.
L	Length (of shaft), ins.
$L_{A,B}$	Length of shaft between sections A and B, ins.
M	Bending moment, lbf.in.
m_B	Mass of the concentrated mass at B, lbf.sec^2/in.
r_B	Eccentricity of mass B about system axis, in.
S	Shear force, lbf.
T	Torque, lbf.in.
t	Time, seconds
$U_{S_{A,B}}$	Displacement at B due to unit shear force at A, in/lbf.
$U_{M_{A,B}}$	Displacement at B caused by unit bending moment acting at A, in/lbf.in.
$V_{S_{A,B}}$	Slope at B due to unit shear force at A, rad/lbf.
$V_{M_{A,B}}$	Slope at B due to unit bending moment acting at A, rad/lbf.in.
x	Distance along axis of shaft, ins.
y	Vertical displacement, ins.
α	Slope $(\frac{dy}{dx})$, radians
β	Torsional deflections, radians
μ	Mass per unit length, lbf.sec^2/in^2
ω	Frequency of bending vibrations, radians/sec.

Introduction

The vibrations of the drive-line of a motor vehicle, with a simple Hotchkiss drive, may be divided broadly into those that involve bodily displacement of the rear axle and those that involve flexure of the rear axle. Vibrations of the second kind, which are the subject of this investigation, are usually at a higher frequency and smaller amplitude and associated more with the interior noise level than the performance or ride of the vehicle. This note reports on the progress of an investigation of theoretical and experimental methods of assessing the flexural vibrations of the drive-line.

It is well known that the flexural vibrations of drive-line are coupled with the vibrations of the engine block, clutch housing, gearbox and gearbox extension. Staffeld, in a 1960 paper to the S.A.E. (Ref.1), showed the effect of this coupling on the natural frequencies and critical speeds of a propshaft. To evaluate the natural frequencies of the drive-line complete, he divides the system at the rear universal joint and equates the boundary conditions at that joint for the two sub-systems. From the rear universal joint forward to and including the power unit was analysed theoretically with a computer programme. The boundary condition for the rear axle assembly was found experimentally by forcing at the universal joint over a range of frequencies. This semi-empirical method of approach has been used by others in the British motor industry.

It is quite obvious that the measurement of the vibrational characteristics of the rear axle obscures the understanding of the problem and reduces the value of analyses at the design stage of the vehicle. For this reason, the first phase of the investigation was concentrated on the problem of obtaining a better understanding of the rear axle assembly. From the beginning it was recognised that parts of the system may not yield to an analytical approach and, in such cases, recourse may be necessary to a semi-empirical method. It seemed possible that the road wheels and tyres would fall into this category. To avoid the introduction of these complexities at an early stage, the rear axle, without the road wheels, springs and shock absorbers, and the propshaft were considered in isolation from the rest of the system. This note is restricted to the work done with this limited objective - other work with a wider objective is also in progress.

Experimental Methods

To excite the free-free mode of flexural vibrations the propshaft and rear axle were suspended by soft rubber bungees from massive I-section beams, see Plates 1 and 2. Isolation from ground disturbances was improved by mounting the beam on rubber mounts at the supporting pedestals. Light aluminium clamps on the shaft or axle tube were used to connect, through a push rod and force transducer, to an electro-magnetic moving-coil vibrator. Vibro-meter piezo-electric force transducers with charge amplifiers were used for all tests.

New and more convenient instrumentation became available during the progress of the work. For this reason the equipment and measuring techniques that were used, particularly in the early stages, are now obsolete. Nevertheless, the methods are outlined for completeness and for reference purposes.

The propshaft was vibrated with a Derritron vibrator controlled by a Dawe 2 phase sweep oscillator and powered by a Derritron 300 watt amplifier. The shaft displacements in response to the excitation were transduced with a Wayne Kerr capacitance probe and meter and the signal was measured with a Bruel and Kjoer valve voltmeter. By a comparison of the signals from the force and displacement transducers in turn with a signal from the main oscillator, with the phase changed by a Dawe variable adaptor, the phase between the forcing and response was found from the difference in setting of the variable phase adaptor. A Lisajou figure technique was used to match the output of the variable phase adaptor with the appropriate signal from the transducer. A block diagram of the instrumentation is given in Fig.1.

Experiments on the rear axle were conducted in two stages: firstly without the half shafts and secondly with the half shafts fitted. The system was vibrated with an E.M.I. vibrator powered by a 1 kilowatt amplifier and controlled by a Solartron decade oscillator. At the early stages of the experiments the response was recorded with displacement transducers, as described for the propeller shaft, but, for high frequencies the output was too small and small piezo-electric accelerometers were found to be more suitable. Signals from the accelerometer, made by Electromechanisms Ltd., and a signal from the force transducer were resolved and compared with the signal from the oscillator by the use of a Solartron resolved component indicator which gave reference and quadrature readings directly for each case.

Analysis of Experimental Data

Some of the problems that arise in the interpretation of resonance tests were discussed by Bishop and Gladwell in a paper to the Royal Society (Ref.2). Since the natural frequencies of the propshaft are well separated, the maximum-amplitude method was thought to be adequate. However, for checking purposes, the phase difference between the forcing and response signals were also plotted. The frequencies of the propshaft where the receptance or displacement per unit force is a maximum and where the phase difference is 90° are tabulated in Table 1.

For the rear axle experiments, the complex receptance was plotted and the frequencies determined by the Kennedy-Pancu method. These values, with the results of the maximum amplitude and 90° phase methods, are tabulated in Table 2.

Theoretical Methods

A. Propeller Shaft

No difficulty was expected with the prediction of the natural frequencies of free-free vibration. Nevertheless, at the very early stages of the investigation, it was thought to be a necessary and worthwhile check on the experimental methods that they should be capable of measuring the natural frequencies and modal shapes of a simple beam or shaft.

For analytical purposes the propshaft was considered to be a simple uniform tube with concentrated point masses at each end to represent the joint yokes and flanges, see Fig.2. The method of analysis is similar to that of the rear-axle and will be discussed under the next heading.

B. Rear Axle

(1) Without the half shafts

For this case the system was represented by a model consisting of simple uniform tubes connecting five point masses A, B, C, D and E, as illustrated by Fig.3. The idealisation of the system for the theoretical treatment of distributed mass and shaft elasticity is illustrated by Fig.4. Masses A and E represent the brake drum assemblies, B and D the spring anchor brackets, and C the differential case, differential gears and a stiffening plate which replaces a sheet metal cover that encloses the gears. The appropriate values of the mass and the angular inertia and, where necessary, the position of the centre of gravity were calculated from the manufacturers drawings.

The chosen method of analysis for the free-free natural frequencies and the modal shape of the axle is an adaption of the Myklestad method (Ref.6) for bending with an allowance for a torsional coupling. Consider a typical element between two stations along the shaft or axle, see Fig.5, with a point mass, and mass moments of inertia at the left hand of a shaft element with flexibility but no mass. Assuming that the motion is simple harmonic, the equations for the displacements, shear forces, moments and torques can be written:-

$$
\begin{aligned}
y_{n+1} &= y_n - \alpha_n L_{n,n+1} + S_n U_{S_{n,n+1}} - M_n U_{M_{n,n+1}} \\
\alpha_{n+1} &= \alpha_n - S_n V_{S_{n,n+1}} + M_n V_{M_{n,n+1}} \\
S_{n+1} &= S_n + m_{n+1} \omega^2 (y_{n+1} + r_{n+1} \beta_{n+1}) \\
M_{n+1} &= M_n - S_n L_{n,n+1} - I_{\alpha,n+1} \omega^2 \alpha_{n+1} \\
\beta_{n+1} &= \beta_n - \frac{T_n}{GI_p} L_{n,n+1} \\
T_{n+1} &= T_n + J_{n+1} \omega^2 \beta_{n+1} + m_{n+1} \omega^2 y_{n+1} r_{n+1}
\end{aligned}
\qquad (1)
$$

Over a length where a uniformly distributed mass is taken to apply, the shaft is assumed to behave according to the classical wave equation for bending, neglecting the effects of angular inertia and transverse shear deformation, that is:

$$
EI \frac{\partial^4 y}{\partial x^4} + \mu \frac{\partial^2 y}{\partial t^2} = 0 \qquad (2)
$$

A solution of the wave equation is used to define the change of displacement, shear force and bending moment along the element, that is:

$$
\begin{aligned}
y &= A \sin ax + B \cos ax + C_e{}^{ax} + D_e{}^{-ax} \\
\alpha &= a(A \cos ax - B \sin ax + C_e{}^{ax} - D_e{}^{-ax}) \\
M &= EIa^2(-A \sin ax - B \cos ax + C_e{}^{ax} + D_e{}^{-ax}) \\
S &= EIa^3(-A \cos ax + B \sin ax + C_e{}^{ax} - D_e{}^{-ax})
\end{aligned}
\qquad (3)
$$

The Myklestad method is given elsewhere (Refs. 3, 4 and 6) and will not be described in detail here. For an element with a uniformly distributed mass, behaving according to equation 3, the values of y, α, S and M at the right hand end are known from previous calculations on elements to the right according to the specified boundary conditions. Substituting these values in equation 3 gives four simultaneous equations that are solved for the coefficients A, B, C and D. With the known coefficients the corresponding values of y, α, S and M can be calculated for the left hand end of the element. These may be the 'starting' values in equation 1 for the next element.

The method requires that trial frequencies of vibration are used and the values adjusted until a 'residual' force or moment becomes zero or negligible. A digital programme has been written in Algol for the analysis of any beam-type structure. A cubic interpolation scheme is used to 'home' quickly on to the frequency where the residual is zero or zero within a pre-set limit. Before calculating and printing out the modal shape at the natural frequency, a check is made to see whether the change of the residual from positive to negative is occurring at a true natural frequency or whether it is an anti-resonance frequency where the residual changes sign between positive and negative infinity.

For the purposes of assessing the relative importance of continuous mass the calculations were repeated, in some cases, with the continuous elements broken down into several discrete point masses connected by massless beams. Also, the effect of the torsional coupling was assessed by comparison of the frequencies with and without the terms of equation 1 that include the angle of twist β or the torque T. Tabulated in Table 2 are the results of these alternatives.

(11) Rear axle with the half shaft fitted

(a) An adaption of Myklestad's Method

Illustrated by Fig.6 is a simplified model of the rear axle with the half shafts fitted so that between 'a' and 'b', and 'c' and 'd' the half shafts are in parallel with the axle tubes. By an adaption of the Myklestad method the parallel systems may be treated by a distribution of the shear force and bending moment between the two paths with end conditions assumed for the half shaft. For a first analysis the assumption is that the half shafts are 'built-in' at each end, that is, the deflections and slopes at the ends are the same as the rear axle tubes at the branching points. For

example, at section 'a' the deflection y_a and the slope α_a will be the same for both paths, say path A and path B. A fraction χ of the shear force S_a will be carried by path A and the remainder $(1 - \chi)$ by path B. Similarly, a fraction Z of the bending moment at 'a' will be carried by path A and a fraction $(1 - Z)$ by path B.

Four pairs of end conditions at 'a' are taken in turn for a calculation by the parallel paths A & B, that is:

(i) $y_{A,a} = y_a$ $\quad y_{B,a} = y_a$

$\alpha_{A,a} = 0$ $\quad \alpha_{B,a} = 0$

$S_{A,a} = 0$ $\quad S_{B,a} = 0$

$M_{A,a} = 0$ $\quad M_{B,a} = 0$

(ii) $y_{A,a} = 0$ $\quad y_{B,a} = 0$

$\alpha_{A,a} = \alpha_a$ $\quad \alpha_{B,a} = \alpha_a$

$S_{A,a} = 0$ $\quad S_{B,a} = 0$

$M_{A,a} = 0$ $\quad M_{B,a} = 0$

(iii) $y_{A,a} = 0$ $\quad y_{B,a} = 0$

$\alpha_{A,a} = 0$ $\quad \alpha_{B,a} = 0$

$S_{A,a} = S_a$ $\quad S_{B,a} = S_a$

$M_{A,a} = 0$ $\quad M_{B,a} = 0$

(iv) $y_{A,a} = 0$ $\quad y_{B,a} = 0$

$\alpha_{A,a} = 0$ $\quad \alpha_{B,a} = 0$

$S_{A,a} = 0$ $\quad S_{B,a} = 0$

$M_{A,a} = M_a$ $\quad M_{B,a} = M_a$

If $(y_{A,b})_y$, $(y_{A,b})_\alpha$, $(y_{A,b})_S$ and $(y_{A,b})_M$

are the displacements at b, by path A, calculated with the boundary conditions (i) to (iv) respectively, then for a linear system the deflection at b may be computed by:

$$y_{A,b} = (y_{A,b})_y + (y_{A,b})_\alpha + \chi\,(y_{A,b})_S + Z\,(y_{A,b})_M \qquad (4)$$

With a similar notation the following equations will apply also:

$$y_{B,b} = (y_{B,b})_y + (y_{B,b})_\alpha + (1 - \chi)(y_{B,b})_S + (1 - Z)(y_{B,b})_M \quad (5)$$

$$\alpha_{A,b} = (\alpha_{A,b})_y + (\alpha_{A,b})_\alpha + \chi\,(\alpha_{A,b})_S + Z\,(\alpha_{A,b})_M \quad (6)$$

and $$\alpha_{B,b} = (\alpha_{B,b})_y + (\alpha_{B,b})_\alpha + (1 - \chi)(\alpha_{B,b})_S + (1 - Z)(\alpha_{B,b})_M \quad (7)$$

With the boundary condition

$$y_{A,b} = y_{B,b} \quad \text{and} \quad \alpha_{A,b} = \alpha_{B,b},$$

equations (4) to (7) are solved for χ and Z. For the particular trial frequency the boundary conditions for the beginning of each path are now known completely so that equations similar to (1) or (3) can be applied to find the values of y, α, S and M at the section 'b', the end of the parallel system.

At a natural frequency the programme computes the values of y and α at suitable points along the axle and half shafts. Computed frequencies for the free-free vibrations of the rear axle with the half shafts fitted are tabulated in Table 2.

TABLE 1

Natural Frequencies of Propeller Shaft (cycles per second)

Theoretical	Experimental					
	At Max. Amplitude			At 90° phase difference		
	Vibrator at:			Vibrator at:		
	Mid-length	End	$\frac{1}{3}$ of length	Mid-length	End	$\frac{1}{3}$ of length
180	196	205	199	194	202	203
588			575			563
		610			607	
			940†		950*	
	1050	1150	1000			1040
1242			1250		1156	1257
	1525†	1450			1462	
	1800†					
2114						

† SMALL PEAK

* NOT A TRUE PHASE DIFFERENCE OF 90°
OR A DISTORTED CURVE

TABLE 2

latural Frequencies of Rear Axle (cycles per second)

Without Half-Shafts						With Half-Shafts			
Theoretical			Experimental			Theoretical	Experimental		
Pure Bending		Bending & Torsion	At Maximum Amplitude	At 90° Phase Difference	Kennedy & Pancu Method	By Myklestad	At Maximum Amplitude	At 90° Phase Difference	Kennedy & Pancu Method
Lumped	Lumped & Continuous								
77	77	77	71	71	71	74	68	68	68
			255						
286	288	285	312	310	310	245	259	258	258
			605			450			
608	612	617	636	634	632	561			
					641	646			
895	900	893				801			

Results

See Tables 1 & 2

Discussion of Results

It would appear, according to the comparison of results in Table 1, that the prediction and measurement of the free-free natural frequencies of a propshaft is more difficult than one might expect. At the fundamental frequency, for example, the difference between the theoretical value and the measured value is about 10%. This difference is somewhat greater than one would expect considering that the analysis takes account of the distributed mass along the shaft and neglects the angular inertia and shear deflections. At the second natural frequency there is a somewhat better comparison - particularly when the vibrator is away from the end of the shaft. At higher frequencies the range of measured values is such that a comparison with the theoretical result has little meaning. It is possible that one or two of the measured resonances at high frequencies are caused by a distortion of the forcing signal and resonance of the forcing overtones with higher modes of vibration of the shaft.

Because the mass of the propshaft is comparatively small, about 15 lbm, and the length is long, about 51 inches, it is possible that the restraints caused by the shaft suspension and the attachment of the vibrator were sufficient to prevent a free-free vibration. This may be particularly so when the vibrator is attached at a point where the angular deflection, due to flexure of the shaft, is appreciable because the method of clamping does not give full freedom of movement in this direction. For future experiments on similar shafts it suggests that more care should be taken to clamp the vibrator in the region of an anti-node and to suspend from the regions of the nodes.

Another possibility was that the 'effective' mass of the moving coil of the vibrator and the light aluminium clamps were sufficient to affect the natural frequency of the propshaft. The calculations were repeated with the effective mass, determined experimentally, positioned at the end of the shaft and at the mid-length. The computed frequencies were as follows:

Mass at End	Mass at mid-length
f_1 = 178 cps	f_1 = 172 cps
f_2 = 585 cps	f_2 = 589 cps
f_3 = 1237 cps	f_3 = 1180 cps
f_4 = 2103 cps	f_4 = 2115 cps

These results partially explain the small differences that are observed when the vibrator is positioned at different places along the shaft but do not account for the significant difference between the measured and calculated frequencies for the fundamental mode. Figure 7 also illustrates that the measured modal shape is somewhat different to the calculated values at the fundamental frequency.

According to the results at the lower frequencies, there is little to choose between the maximum amplitude method and 90° phase difference for the natural frequencies of a propshaft in isolation. At frequencies of about 1000 cycles per second and higher, however, the distortion of the phase plots suggest that Kennedy-Pancu receptance plots may be worthwhile.

B. Rear Axle

In general, the agreement between the experimental and the theoretical results for the rear-axle is better than that for the propeller shaft. It would be expected that the restraints of the suspension and vibrator would be far less significant for the more massive system. The main difficulty in the assessment of the validity of the theoretical model is the lack of experimental data at frequencies above the third mode of the rear axle without the half-shafts and above the second mode when the half-shafts are fitted. All attempts to excite resonances at higher frequencies have so far been unsuccessful.

Where a comparison is possible the differences between the theoretical and experimental results are comparatively small. The measured fundamental frequency is about 6 cycles per second or 8 percent less than the calculated value. The most likely explanation of this difference is the inadequacy of the theoretical model to allow for the flexibility of the differential casing. This flexibility could be assessed by a simple bending test of a casing which is similar to the design shape and casting thickness. If the assessment is to be complete at the design stage or a bending test is impractical, a useful estimate could be made by finite element analyses as used for bell housings (Ref.5). Fortunately, the accuracy required of the estimate of the flexibility of a relatively stiff member is not great.

For the second mode of vibration the calculated frequencies are lower, but not greatly so, than the measured values. Bending across the differential casing is not greatly significant for the second mode because the node is near to the mid-length of the axle, see Figure 20. Low values are usual for a lumped mass model of a continuous system. On the other hand

the allowance for the continuous mass of the axle tubes in the calculation only alters the calculated frequency by 2 cycles per second or less than 1 percent relative to the value when the tube is considered as several lumped masses. A likely explanation of the discrepancy is the errors that arise in the estimation of the masses and angular inertias of a complex shape, such as the differential casing, and the stiffness of the axle tubes in the region of the casing, brake drum, and spring anchor brackets.

At the third mode of vibration, where one would expect the flexibility of the differential casing to become significant again, the theoretical and experimental values for the rear axle without the half-shafts compare very closely - within about 3%. There is little doubt that this accuracy is fortuitous and that two or more errors are tending to cancel at this frequency in particular. One would expect to find greater discrepancies at high frequencies as the walls of the differential casing etc. become more significant in the modal shape of the vibration.

Referring now to the theoretical analyses, it would seem that the distribution of mass along the axle is only slightly significant at high frequencies and a negligible effect at low frequencies. The inclusion of a torsional coupling, present as a consequence of the offset of the centres of gravity from the bending axis, also has only a small effect for this particular axle. Torsional coupling for the first modes of vibration is exhibited by a bodily roll or 'nodding' of the axle about the polar axis of the axle tubes. In the installed situation this motion would be restrained by the road springs and wheels.

Although the parallel system chosen to represent the half-shafts has yet to be confirmed by experimental results, the theoretical results suggest strongly that the half-shafts have a very significant effect on the vibrations of the system. For the particular axle, see Appendix 1 for the dimensions, the half-shafts tend to vibrate in phase with the axle at the fundamental and second mode of vibration. Above the second frequency the half-shafts exhibit motion which is out-of-phase with the axle. Compared with the axle alone many other natural frequencies are introduced to the system above the second mode of vibration

When attempts were made to simplify the model by ignoring the effects of the spring anchor brackets the fundamental frequency and the second natural frequency were not affected greatly but the higher frequencies were changed appreciably. This suggests that care should be taken to avoid over-simplified models that could be misleading.

Conclusions

Vibrating a propeller shaft, in particular, has shown that the measurement of the free-free frequencies and the modal shape is more difficult than one might expect. Great care is required, particularly for a low mass system, to avoid introducing extraneous constants by the supports or the connection to the vibrator. Where possible the vibrator should be placed at or near an anti-node and the suspensions at or near the nodes for the particular mode of vibration. A forcing signal which is free from distortion is essential if confusion from the break through of higher harmonics is to be avoided.

The natural frequencies measured up to now are separated sufficiently to make the Kennedy-Pancu method unnecessary. At the higher frequencies, and for more complex systems, however, where the resonances become closer the value of the method becomes greater. It should be retained in subsequent work for this reason.

It seems evident, at least from theoretical results, that the half-shafts cause many complex modes of vibration of the rear axle system. Although much has yet to be done before the theoretical model can be used with confidence to predict the behaviour of the system when the rear axle is installed in the vehicle, more attention to the stiffness of the half-shaft and axle tubes at the design stage may be very advantageous in moving the resonances to higher frequencies or de-tuning the system from a forcing frequency that is particularly troublesome.

Work in Progress

It is well known that the tyre of a road wheel is a very complex non-linear structure which imposes its own characteristics on the displacements and loads transmitted from the road surface to the axle. How the tyre restrains an axle when the axle is vibrating with a small amplitude is not known. The restraint may be negligible. To check this possibility, a rig has been designed for the direct measurement of the receptances at the rim of a tyre when the wheel oscillates at a small amplitude at various frequencies. In the early stages a solid disc will be used in place of the wheel to avoid wheel resonances. At a later stage the wheel will be isolated for a check on its natural frequencies.

A digital programme is being developed for the analysis of leaf springs and their effect when these are coupled with the axle system. A

similar treatment will be used for the coupling of the axle to the suspension linkage, where this is necessary. When the rear axle system is complete the coupling with the propshaft and power unit will be included in the calculation.

References

1	Staffeld,S.E.	Computer Analysis of Automotive Drivetrains S.A.E. paper 127C and 1960 Transactions.
2	Bishop,R.E.D. & Gladwell,G.M.L.	An Investigation into the Theory of Resonance Testing Proc. of Royal Society, Vol.255, 17th Jan, 1963
3	Stanghan,R.M. & Joyce,B.C.	Prediction by Digital Computer of Resonances in Beam-Like Components Advances in Automobile Engineering (Part III), Pergamon Press
4	Barrett,E.J.	Bending Vibrations of a Crankshaft A.S.A.E. Thesis, 1967
5	Wagle,V.M.	Bending Stiffness of a Bell Housing A.S.A.E. Thesis, 1968
6	Myklestad,N.O.	Fundamentals of Vibration Analysis McGraw-Hill Book Co.

List of Figures

continued...

List of Figures - continuation

APPENDIX I

SYSTEM PARAMETERS

(A) REAR AXLE

Masses (lb. sec^2/in)

Brake Assembly (Right-hand)	0.0161
Brake Assembly (Left-hand)	0.0160
2 Brake Drums	0.0460
4 Bolts (Brake drum to axle shaft)	0.00014
Diff-case plus Rear Cover	0.1200
Axle Tube Assembly (Right-hand)	0.0219
Axle Tube Assembly (Left-hand)	0.0232
Half-shaft (Right-hand)	0.0142
Half-shaft (Left-hand)	0.0156
Rear Spring Anchor	0.00568
Length of Half-shaft (Right-hand)	19.65 ins
Length of Half-shaft (Left-hand)	21.55 ins

Dimensions (ins)

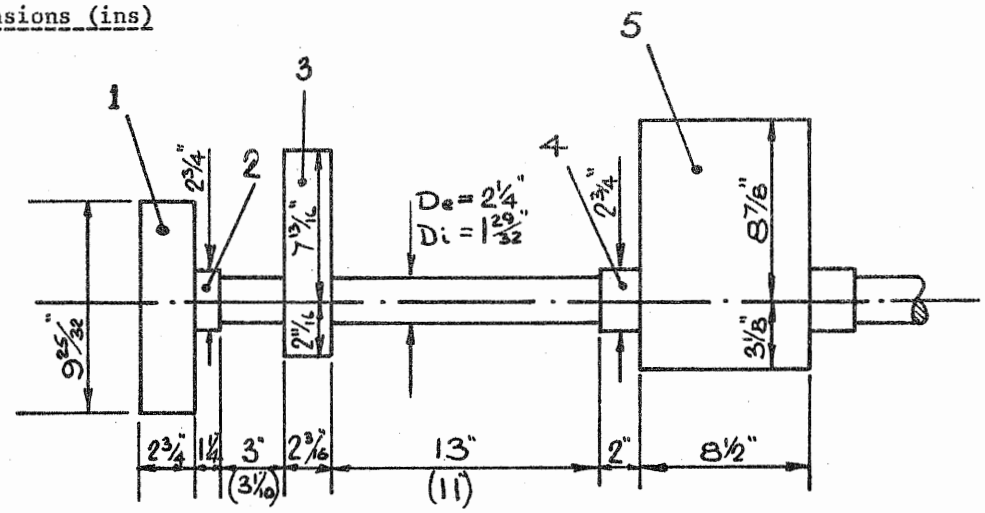

Figures in brackets denote dimensions of identical element on right-hand side of the system, where this is different from left-hand element shown in the Fig.

Mass No	Mass (lb.sec^2/in)	J (lb.sec^2.in)	I_α (lb.sec^2.in)	Eccentricity, r (ins)
1	0.03914	0.46100	0.25500	0.0
2	0.00171	0.00370	0.00150	0.0
3	0.00568	0.05092	0.00148	2.2
4	0.00634	0.01200	0.01245	0.0
5	0.12000	0.80490	0.42300	3.0

(B) PROPSHAFT

Length (centre of front yoke to centre of rear yoke)	51 ins
External Diameter	3 ins
Internal Diameter	2.872 ins
Weight	15.1 lb.

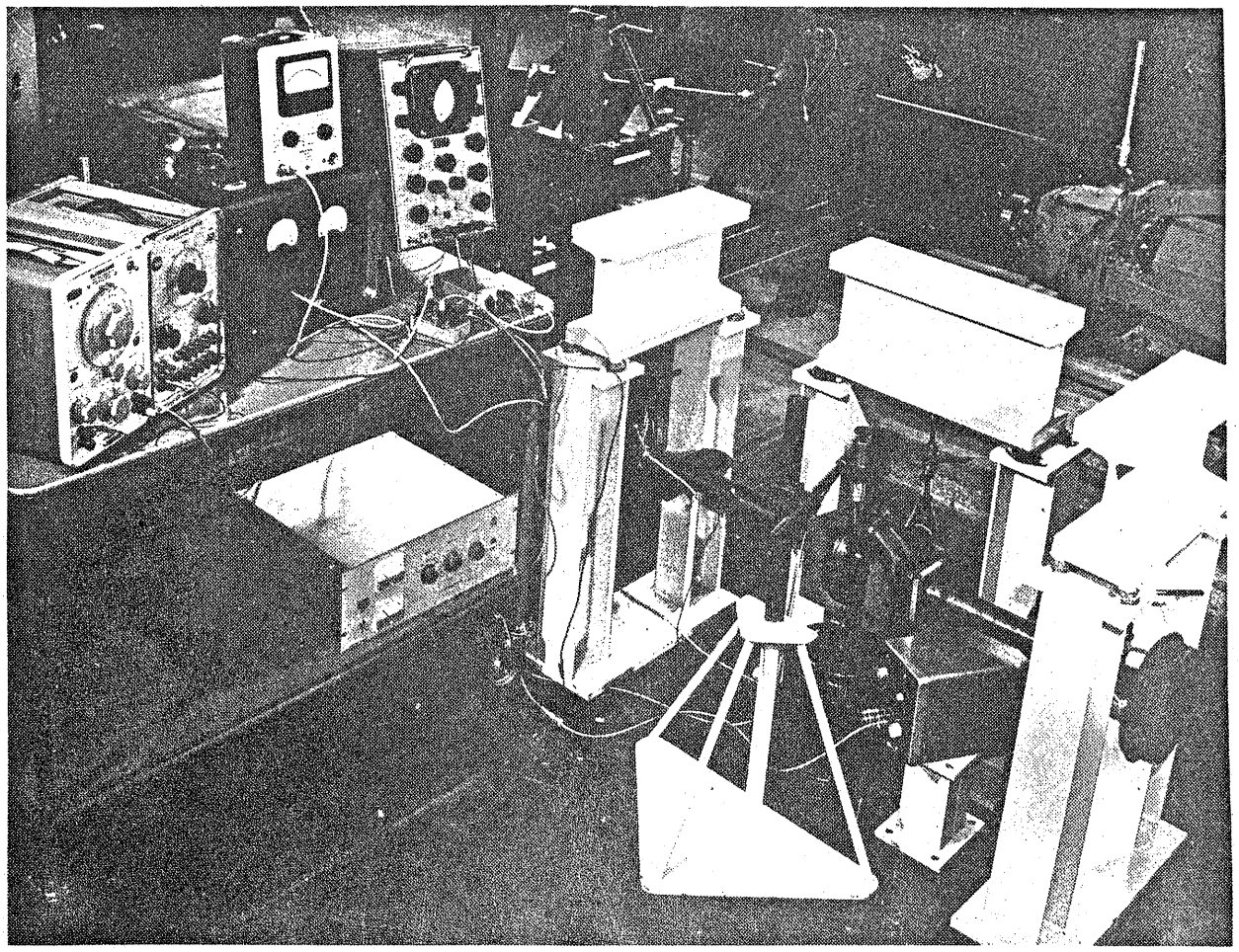

PLATE 1

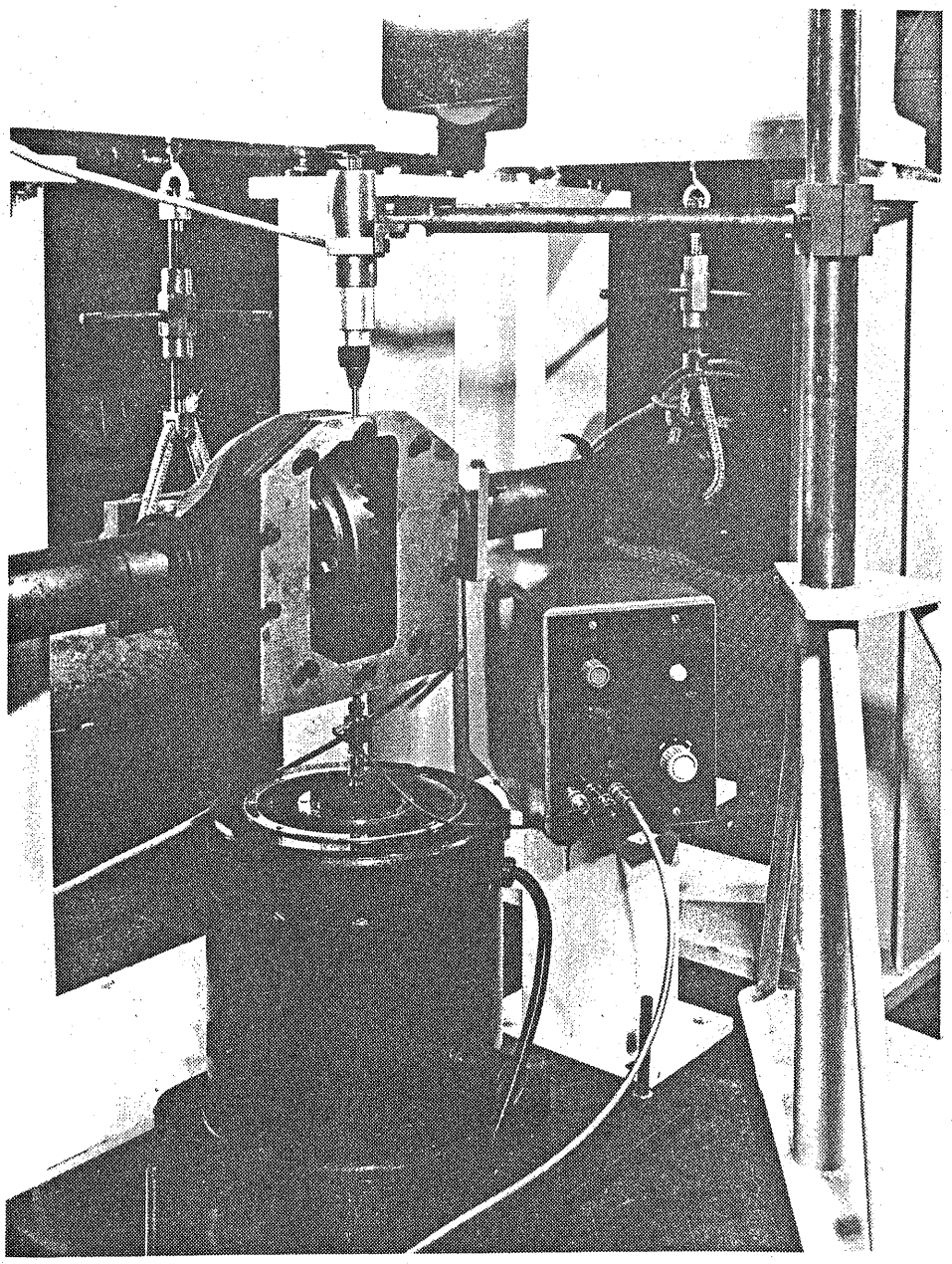

PLATE 2

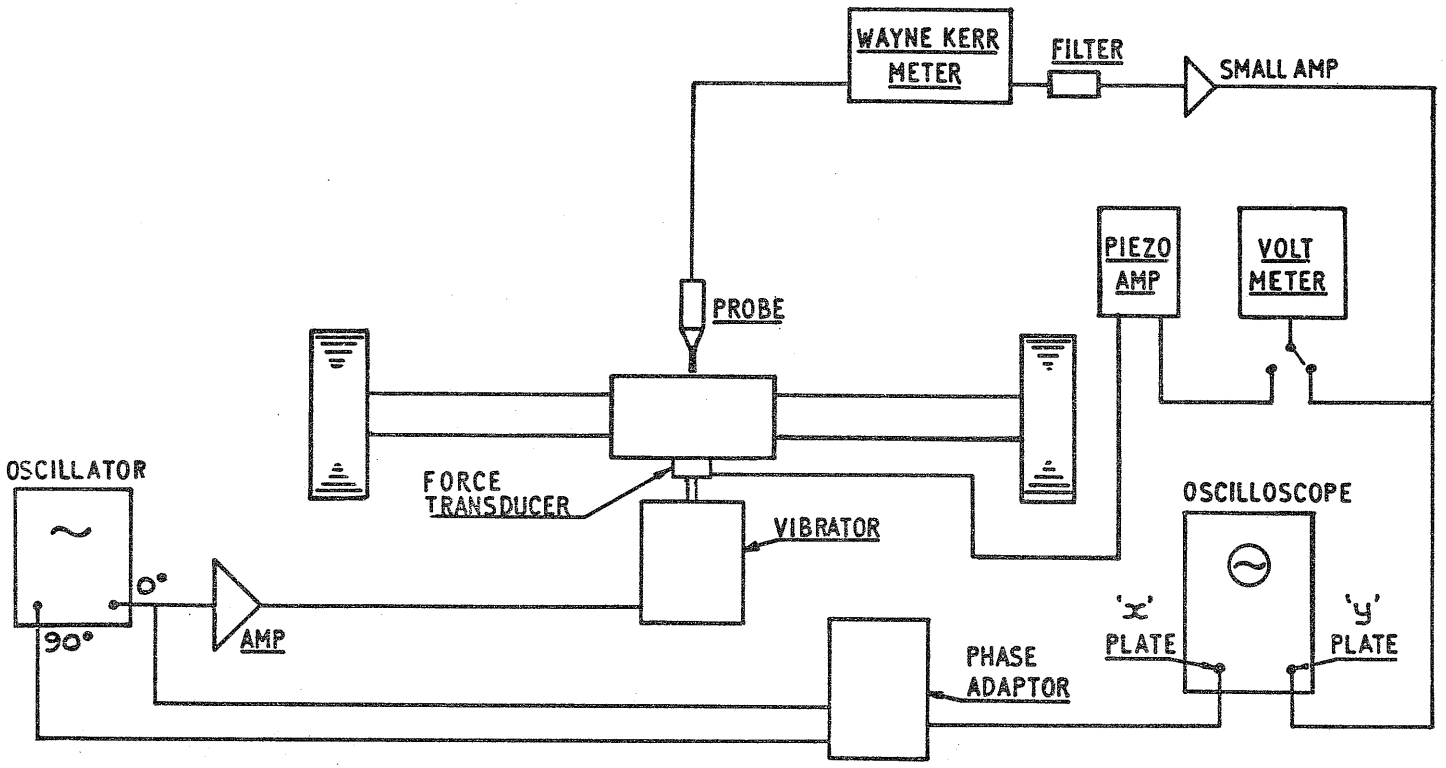
WAYNE KERR METER
FILTER
SMALL AMP
PIEZO AMP
VOLT METER
PROBE
OSCILLATOR
FORCE TRANSDUCER
VIBRATOR
OSCILLOSCOPE
0°
90°
AMP
'x' PLATE
'y' PLATE
PHASE ADAPTOR

FIG. 1

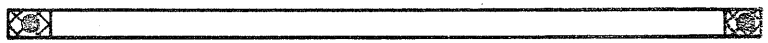

fig 2

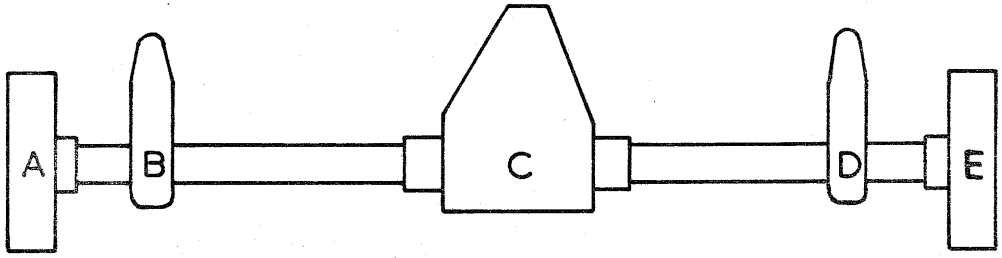

fig 3

fig 4

- concentrated mass
- massless and perfectly rigid length of shaft
- massless but elastic length of shaft
- length of shaft with uniformly distributed mass and elasticity

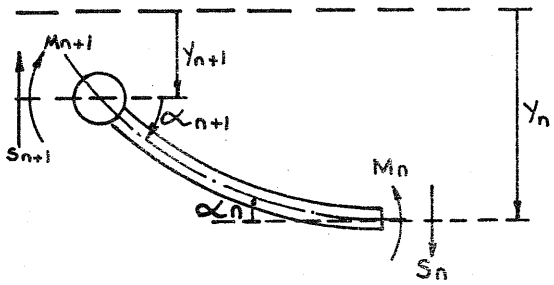

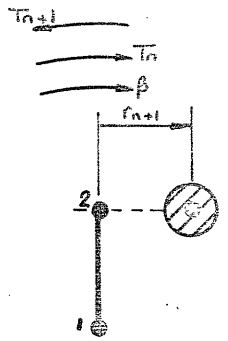

fig 5

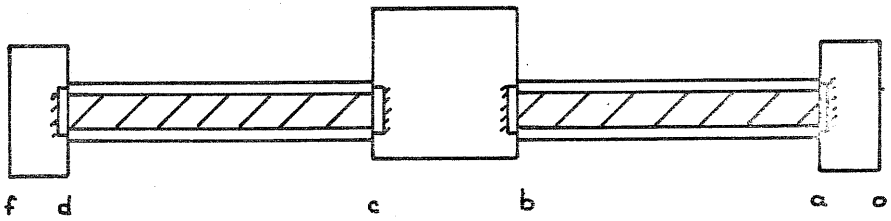

fig 6

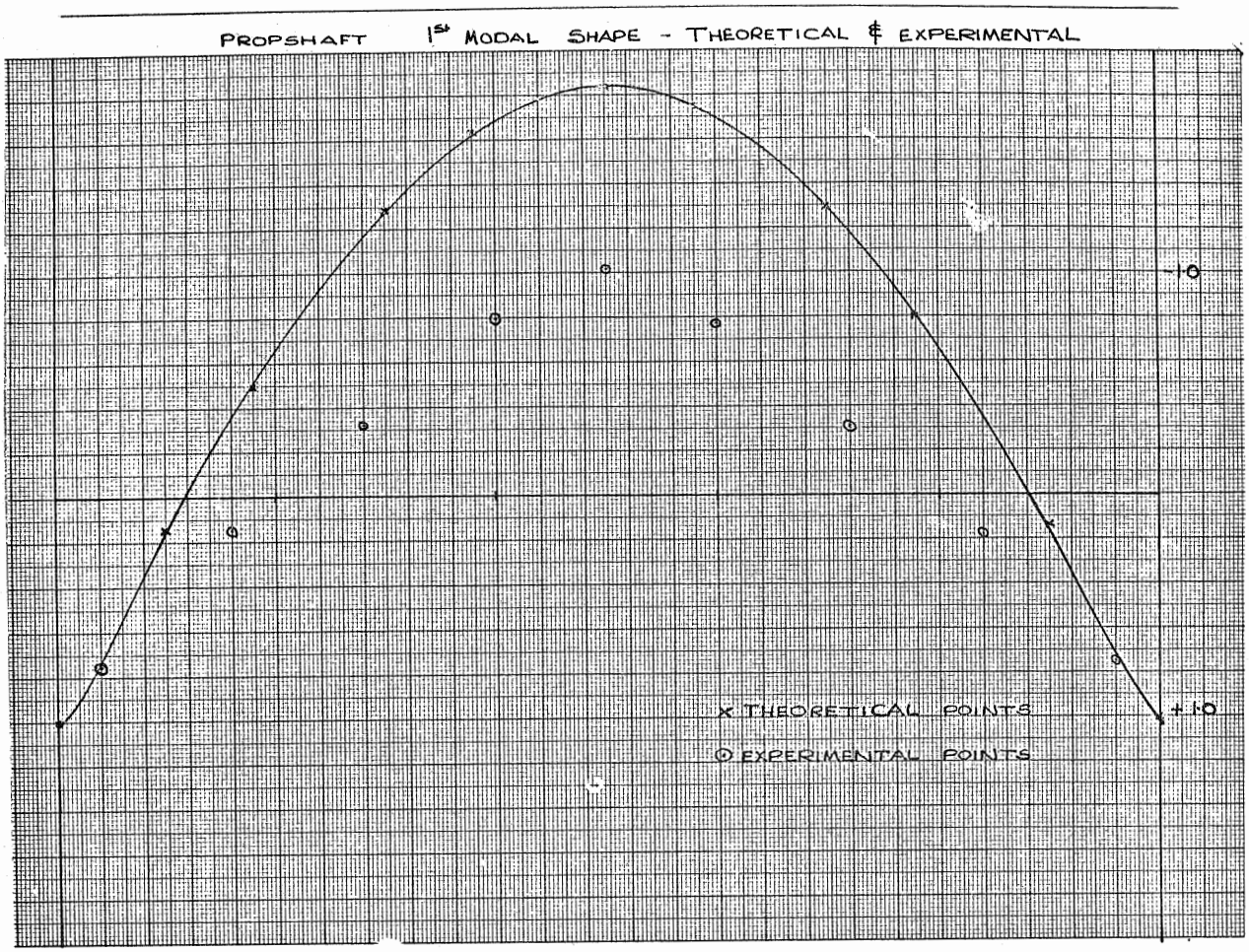
PROPSHAFT 1ST MODAL SHAPE - THEORETICAL & EXPERIMENTAL
-1·0
+1·0
X THEORETICAL POINTS
⊙ EXPERIMENTAL POINTS

FIG 7

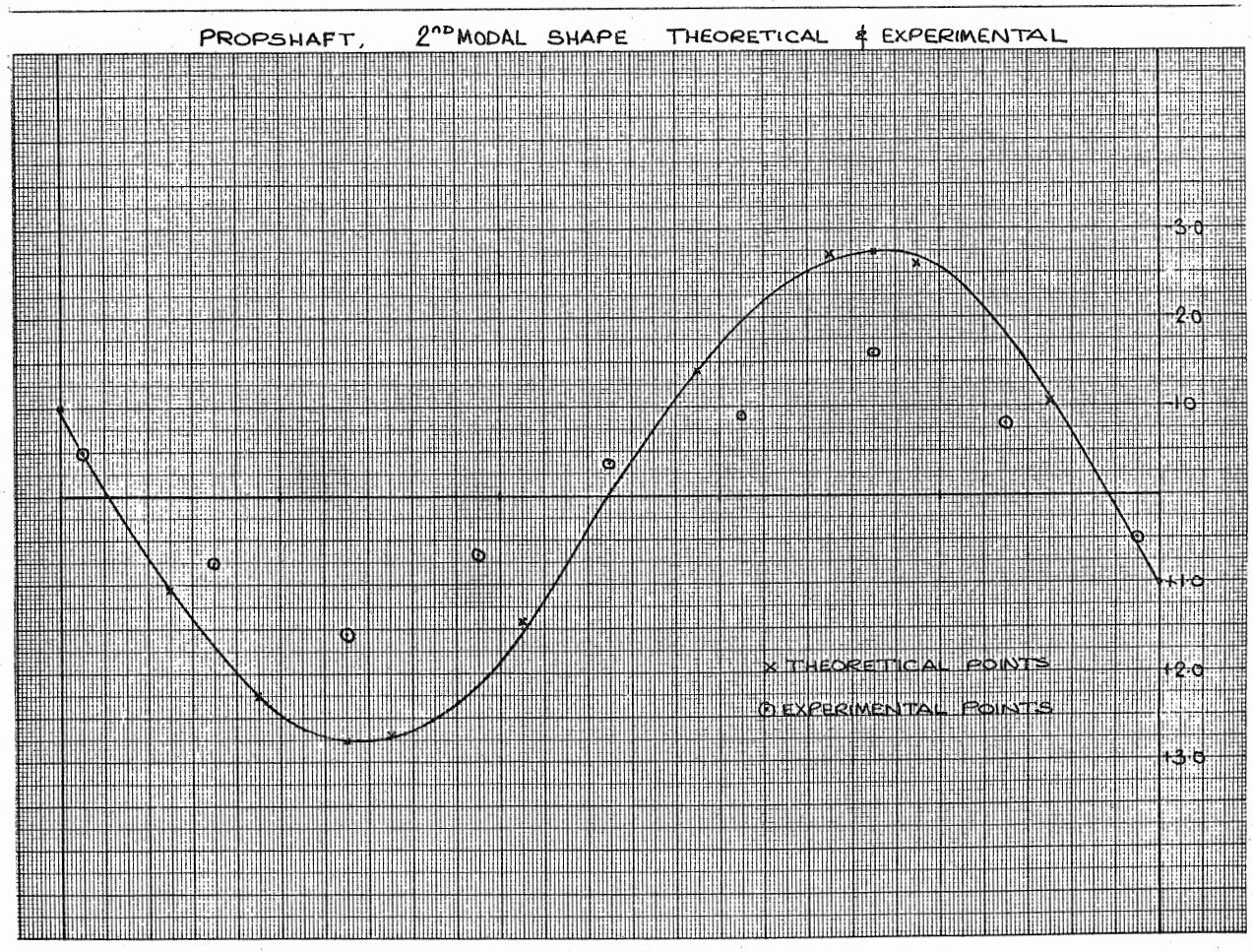
PROPSHAFT, 2ND MODAL SHAPE THEORETICAL & EXPERIMENTAL
-3·0
-2·0
-1·0
+1·0
+2·0
+3·0
X THEORETICAL POINTS
⊙ EXPERIMENTAL POINTS

FIG 8

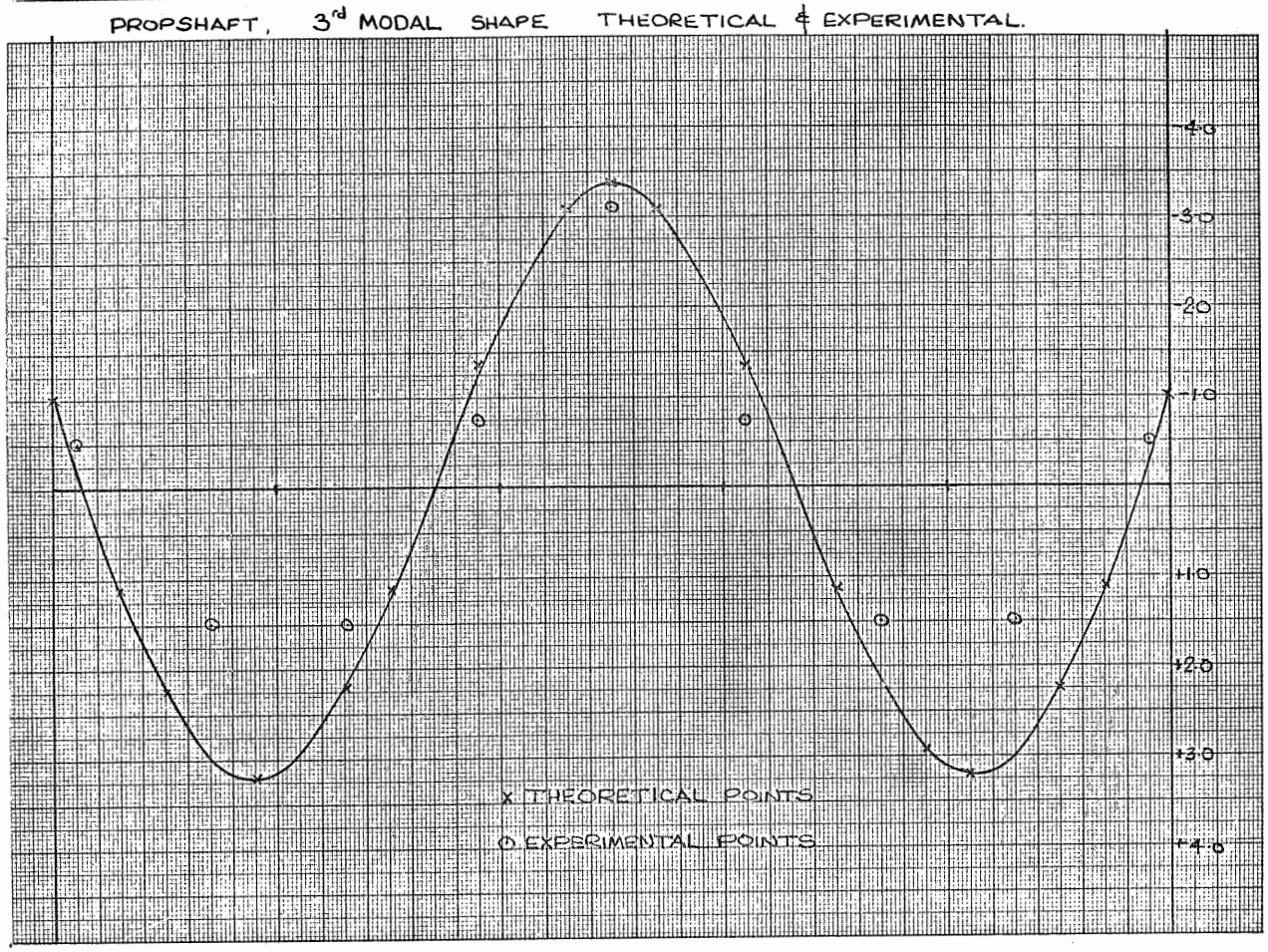
PROPSHAFT, 3rd MODAL SHAPE THEORETICAL & EXPERIMENTAL.
-4·0
-3·0
-2·0
-1·0
+1·0
+2·0
+3·0
+4·0
X THEORETICAL POINTS
O EXPERIMENTAL POINTS

FIG 9

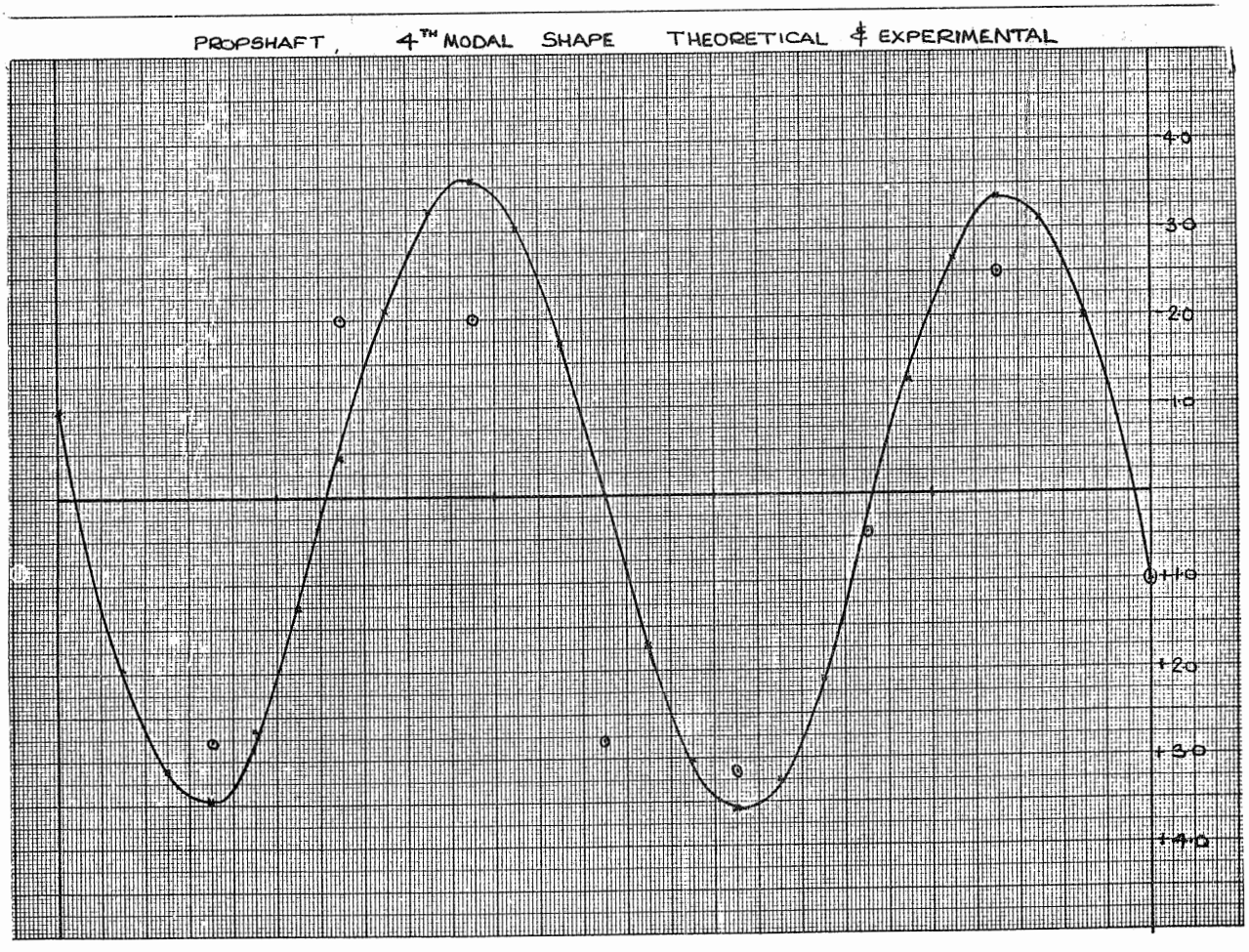
PROPSHAFT, 4TH MODAL SHAPE THEORETICAL & EXPERIMENTAL
-4·0
-3·0
-2·0
-1·0
+1·0
+2·0
+3·0
+4·0

FIG 10

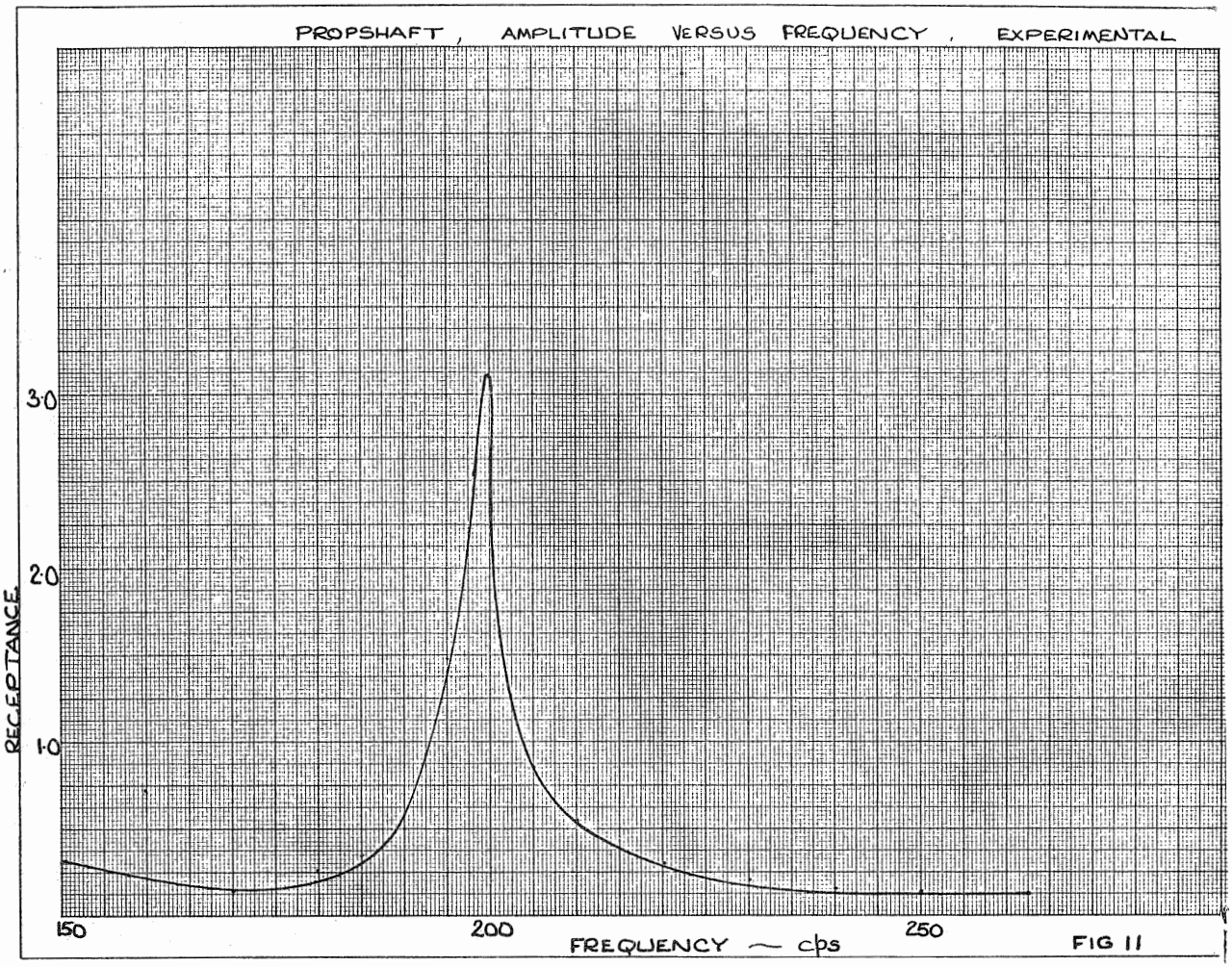
PROPSHAFT, AMPLITUDE VERSUS FREQUENCY, EXPERIMENTAL
RECEPTANCE
3·0
2·0
1·0
150
200
250
FREQUENCY ~ cps

FIG 11

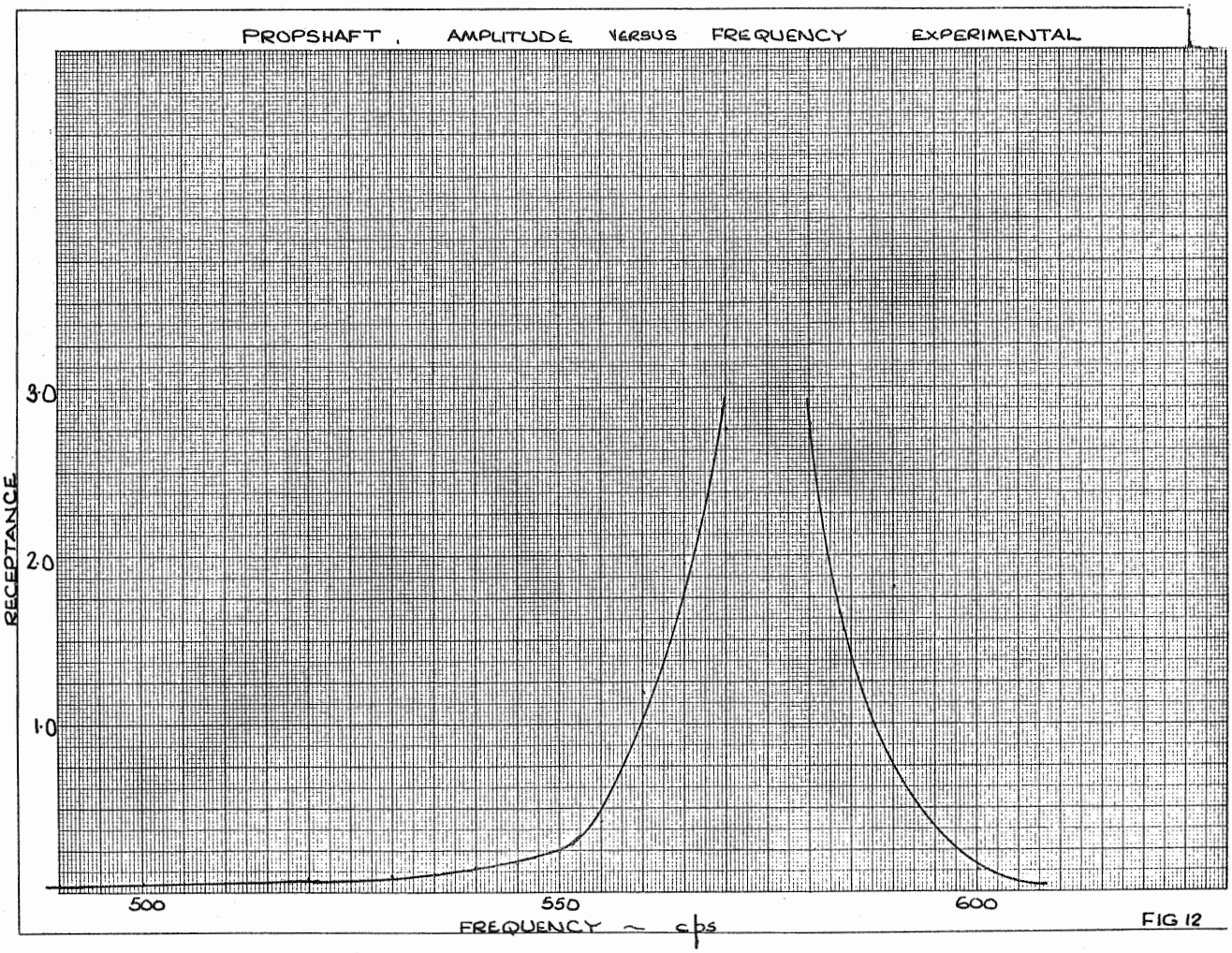
PROPSHAFT, AMPLITUDE VERSUS FREQUENCY EXPERIMENTAL
RECEPTANCE
3·0
2·0
1·0
500
550
600
FREQUENCY ~ cps

FIG 12

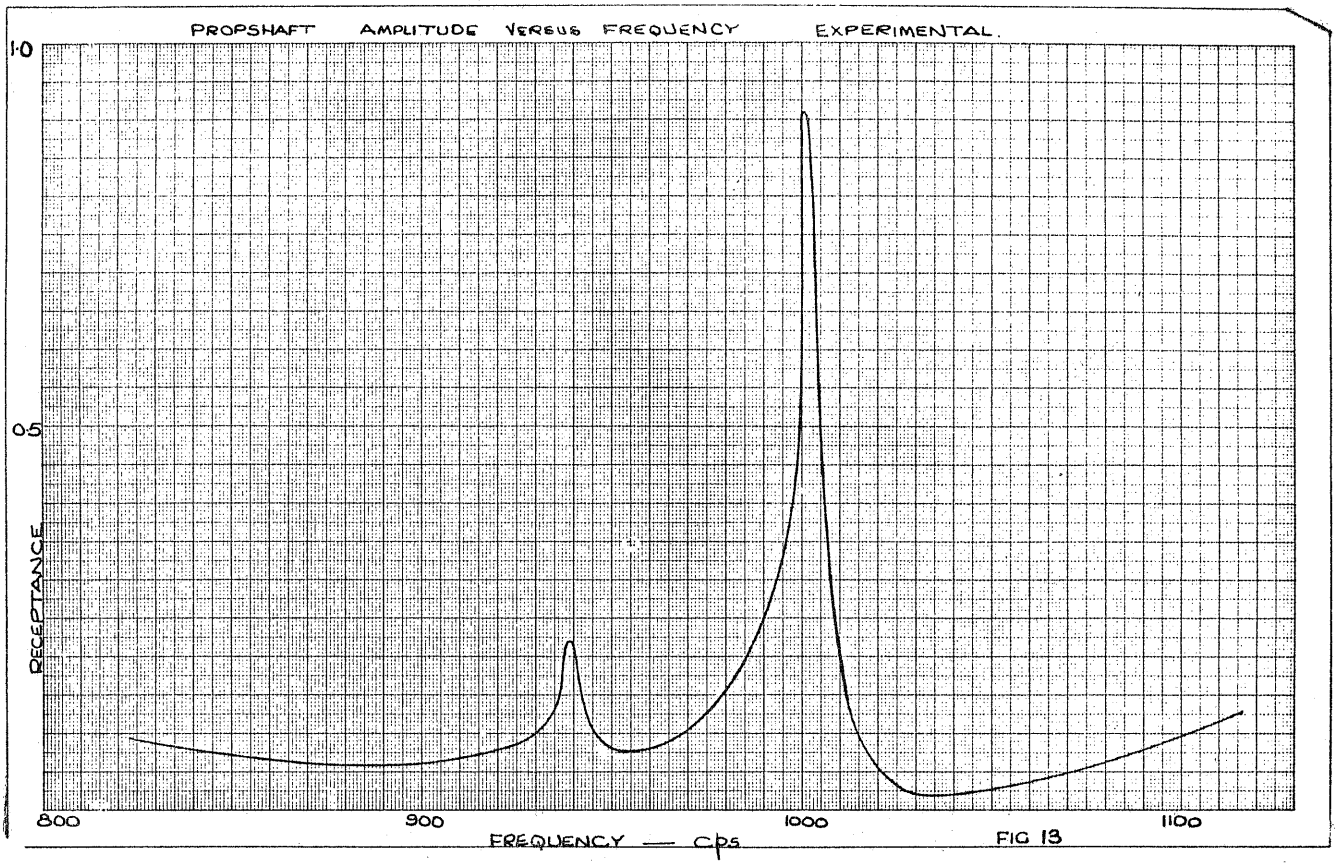
PROPSHAFT AMPLITUDE VERSUS FREQUENCY EXPERIMENTAL.
1·0
0·5
RECEPTANCE
800
900
1000
1100
FREQUENCY — cps

FIG 13

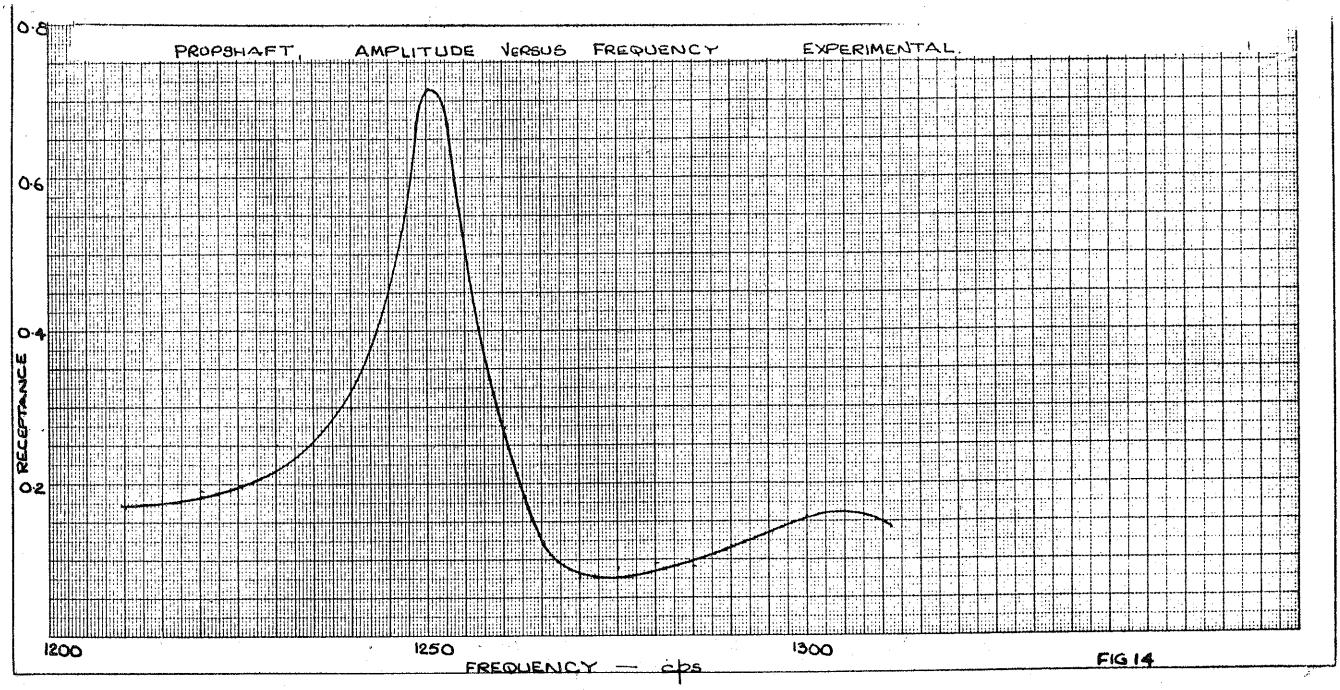
PROPSHAFT, AMPLITUDE VERSUS FREQUENCY EXPERIMENTAL.
0·8
0·6
0·4
RECEPTANCE
1200
1250
1300
FREQUENCY — cps

FIG 14

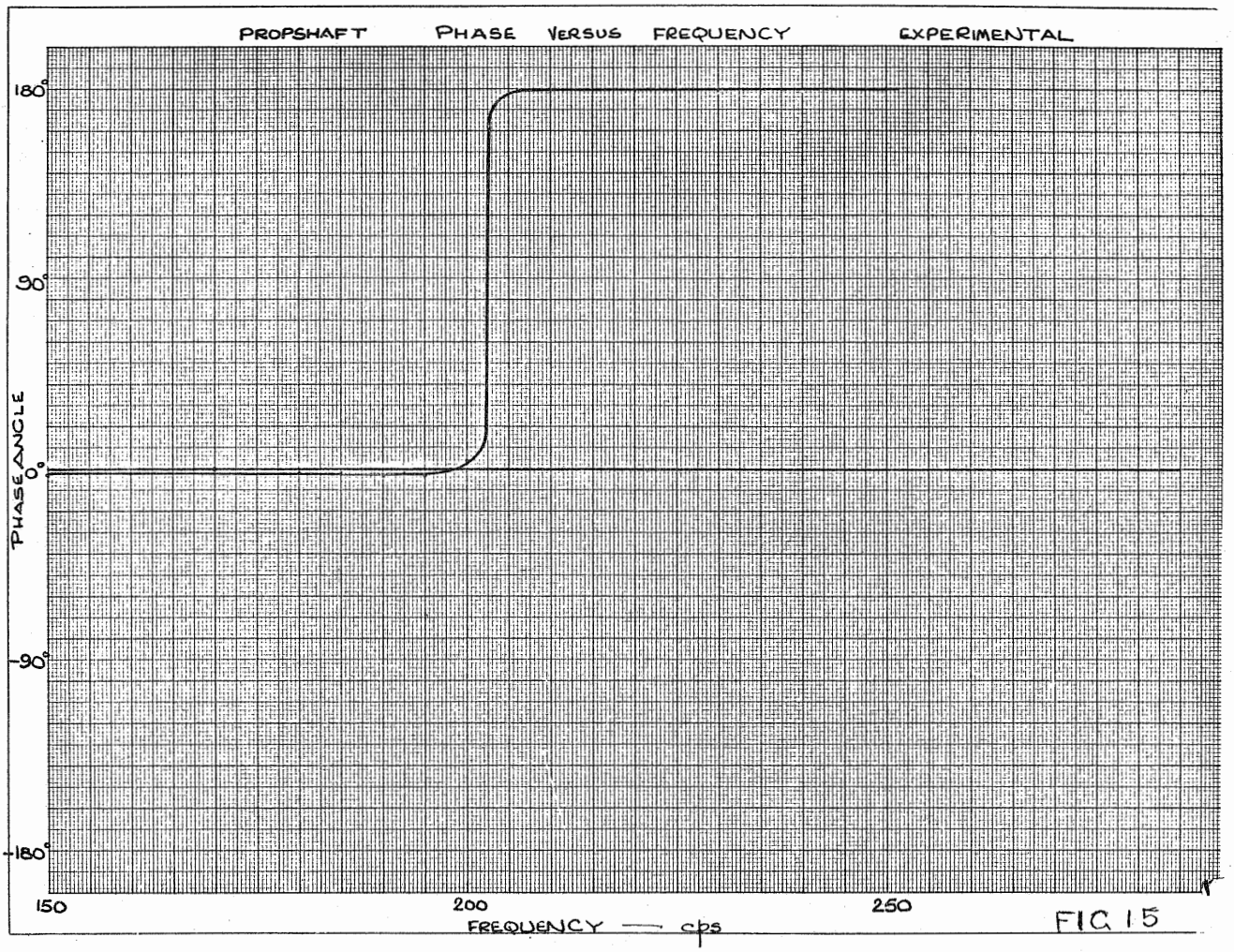

FIG 15

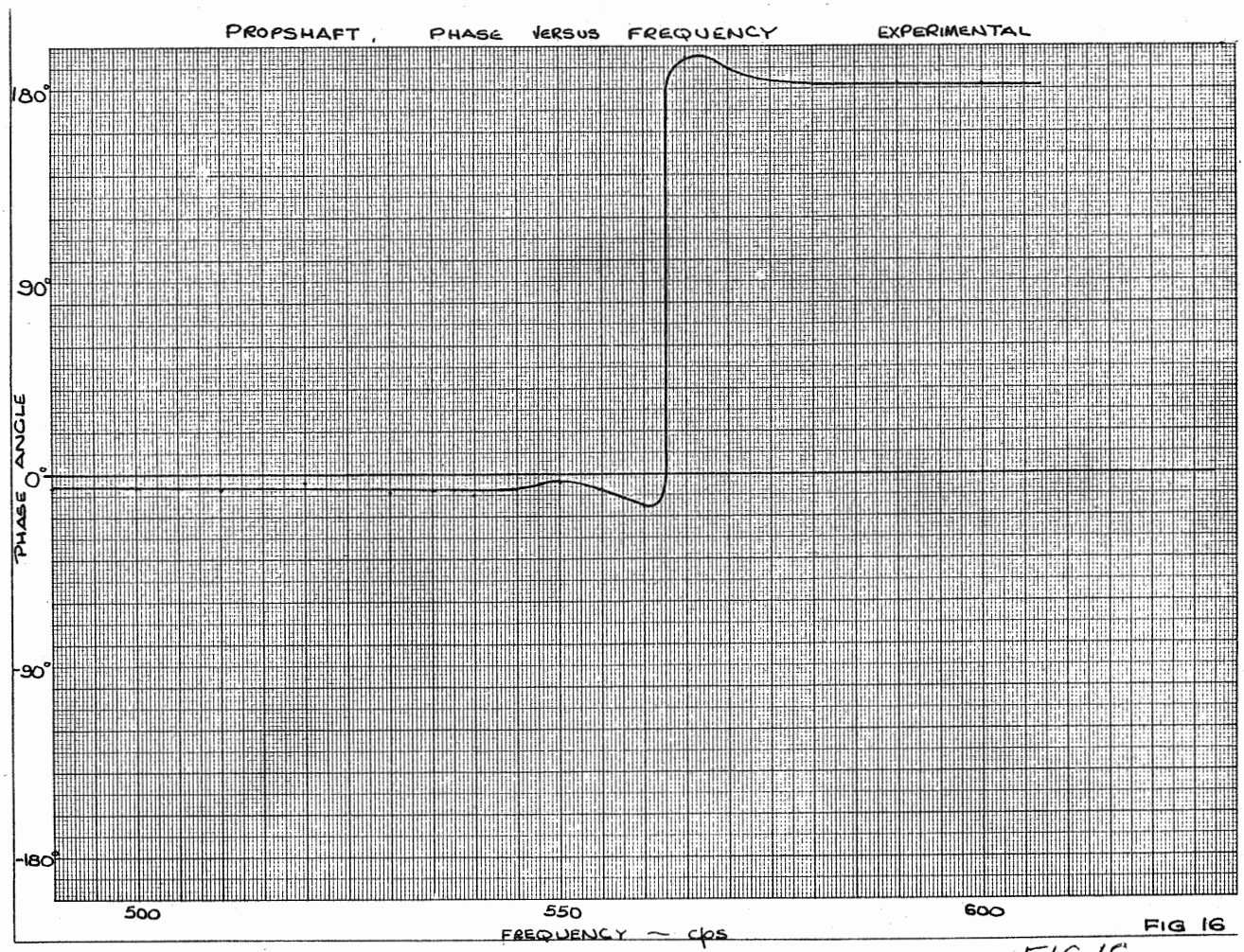

FIG 16

FIG 16

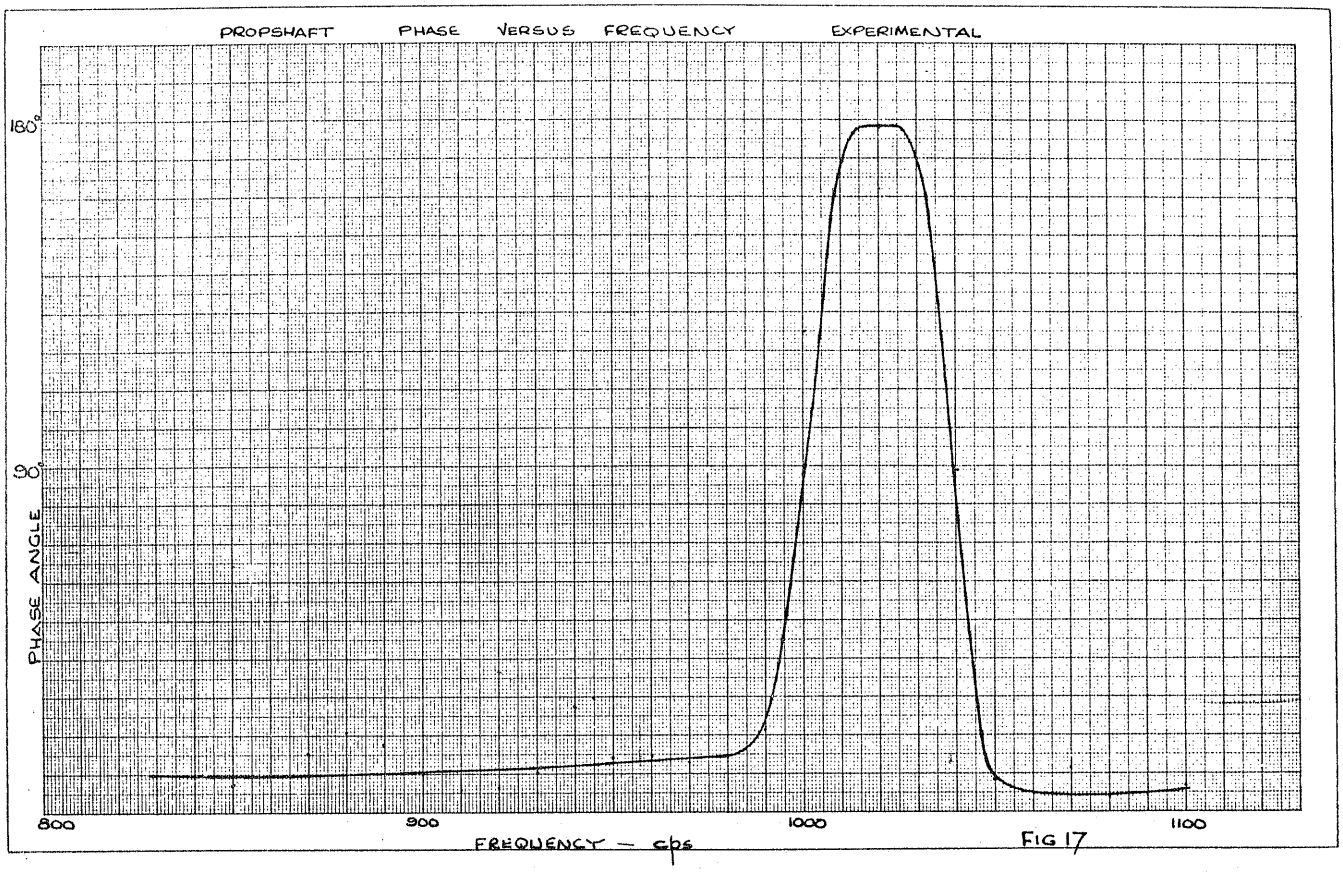
PROPSHAFT PHASE VERSUS FREQUENCY EXPERIMENTAL
180°
90°
PHASE ANGLE
800
900
1000
1100
FREQUENCY — cps

FIG 17

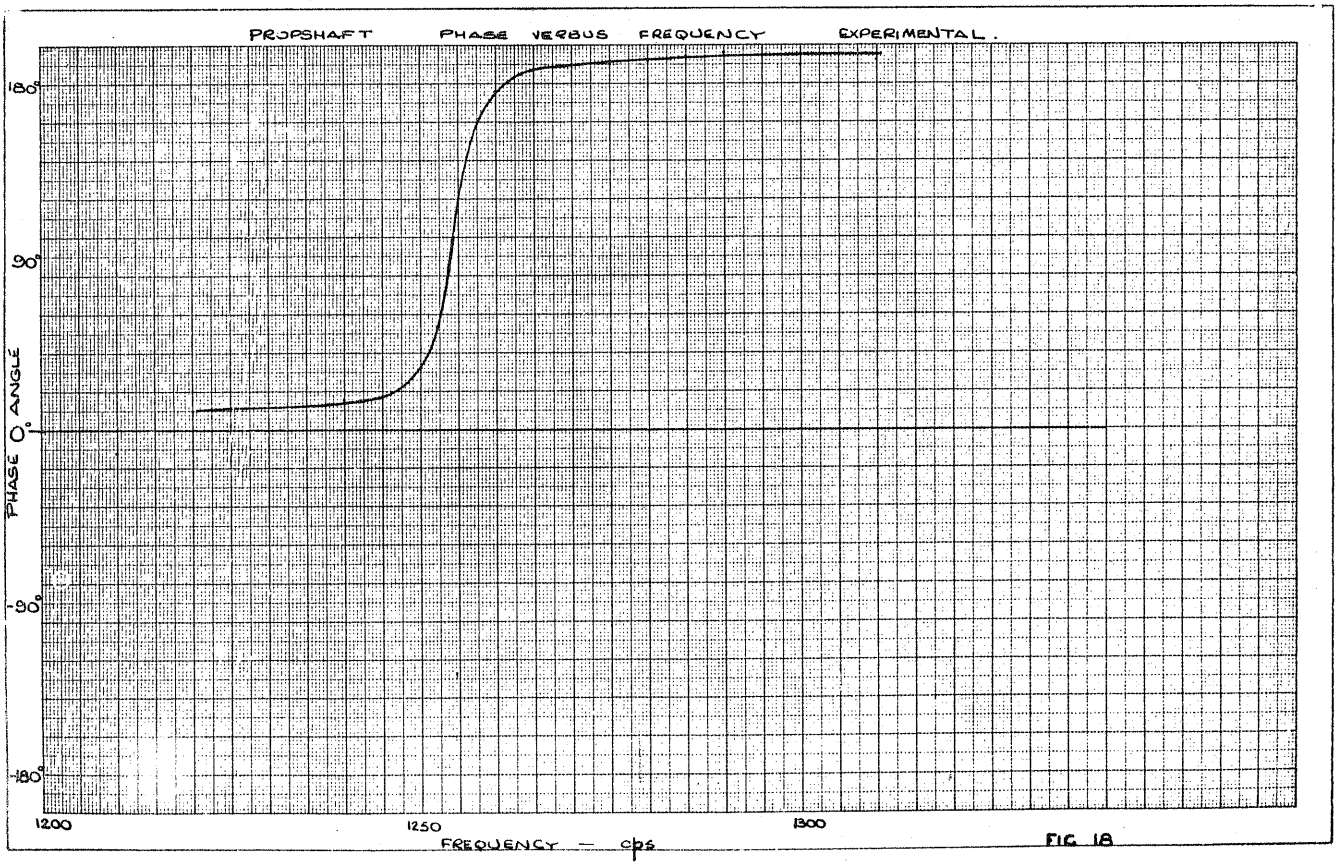
PROPSHAFT PHASE VERSUS FREQUENCY EXPERIMENTAL.
180°
90°
PHASE 0° ANGLE
-90°
-180°
1200
1250
1300
FREQUENCY — cps

FIG 18

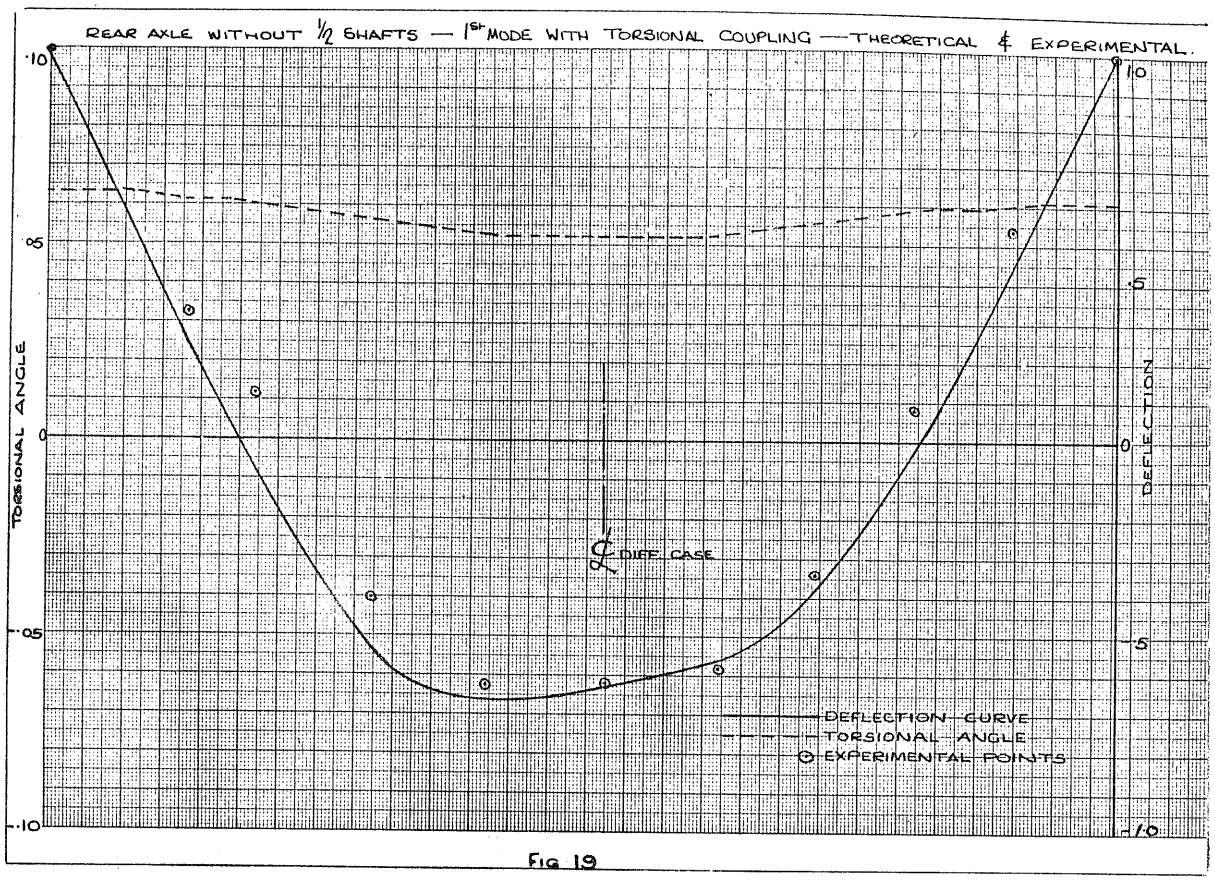
REAR AXLE WITHOUT ½ SHAFTS — 1st MODE WITH TORSIONAL COUPLING — THEORETICAL & EXPERIMENTAL.
TORSIONAL ANGLE
DEFLECTION
·10
·05
0
·05
·10
1·0
·5
0
·5
1·0
℄ DIFF. CASE
DEFLECTION CURVE
TORSIONAL ANGLE
EXPERIMENTAL POINTS

FIG 19

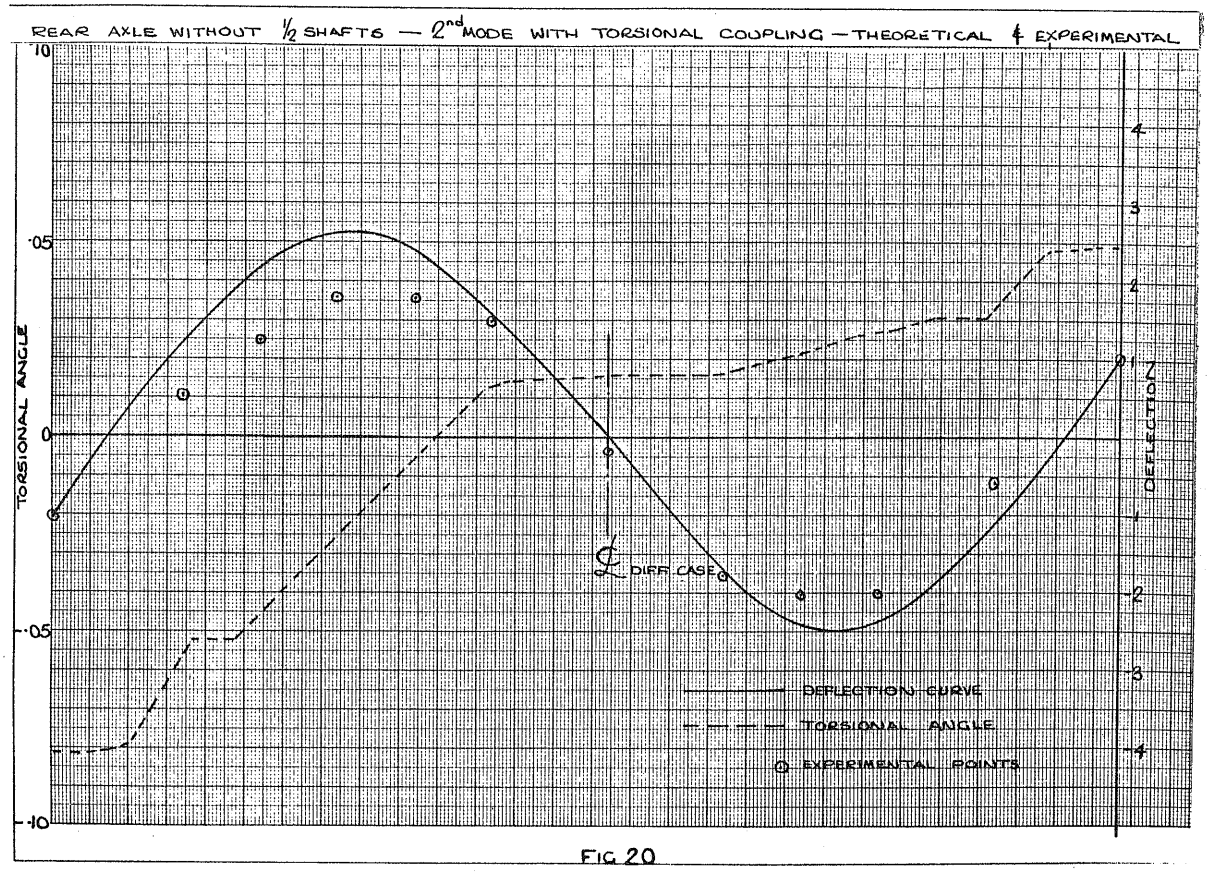
REAR AXLE WITHOUT ½ SHAFTS — 2nd MODE WITH TORSIONAL COUPLING — THEORETICAL & EXPERIMENTAL
TORSIONAL ANGLE
DEFLECTION
·10
·05
0
·05
·10
4
3
2
1
2
3
4
℄ DIFF. CASE
DEFLECTION CURVE
TORSIONAL ANGLE
EXPERIMENTAL POINTS

FIG 20

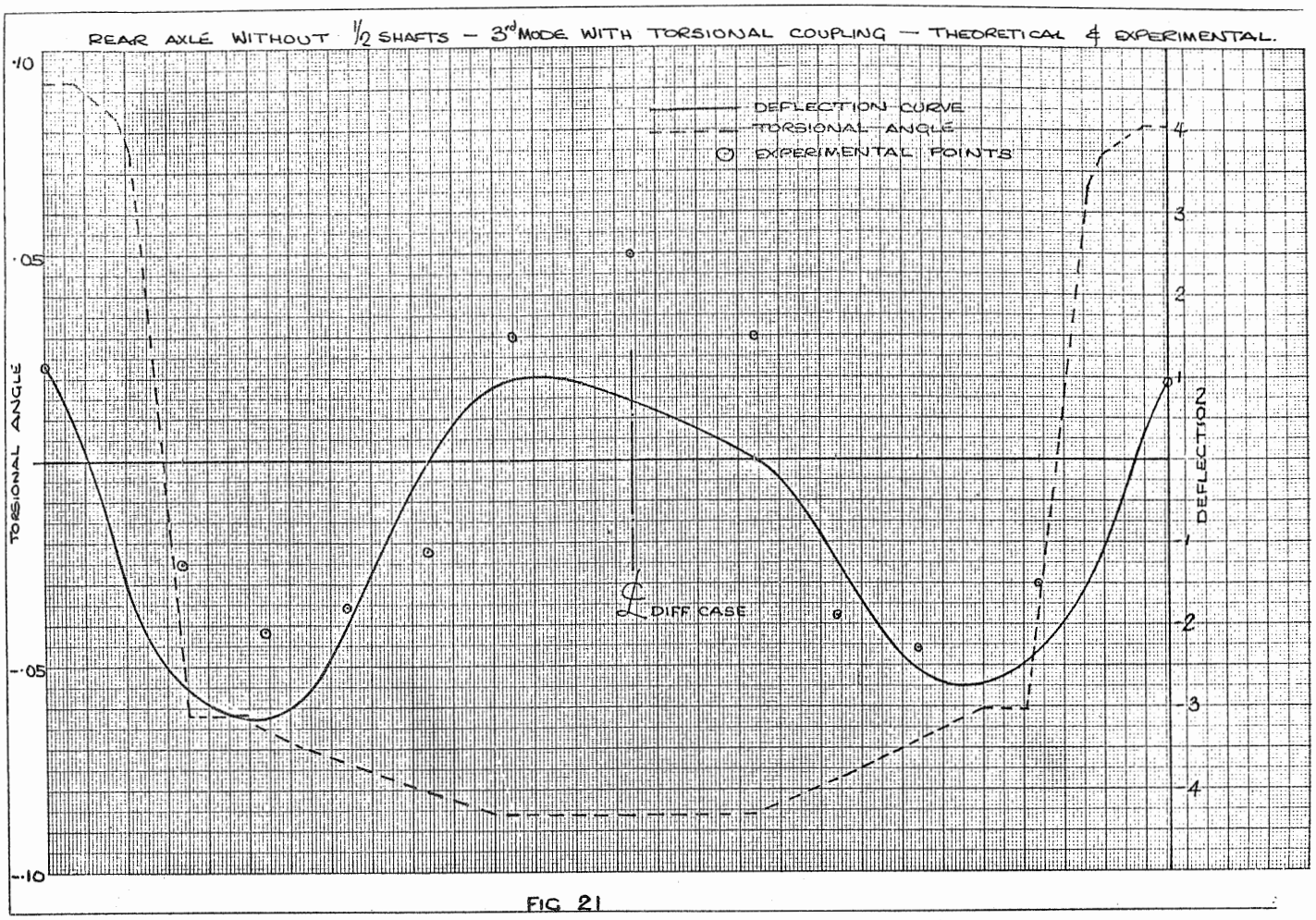
REAR AXLE WITHOUT ½ SHAFTS – 3rd MODE WITH TORSIONAL COUPLING – THEORETICAL & EXPERIMENTAL.
DEFLECTION CURVE
TORSIONAL ANGLE
EXPERIMENTAL POINTS
TORSIONAL ANGLE
DEFLECTION
·10
·05
-·05
-·10
4
3
2
1
-1
-2
-3
-4
℄ DIFF CASE

FIG 21

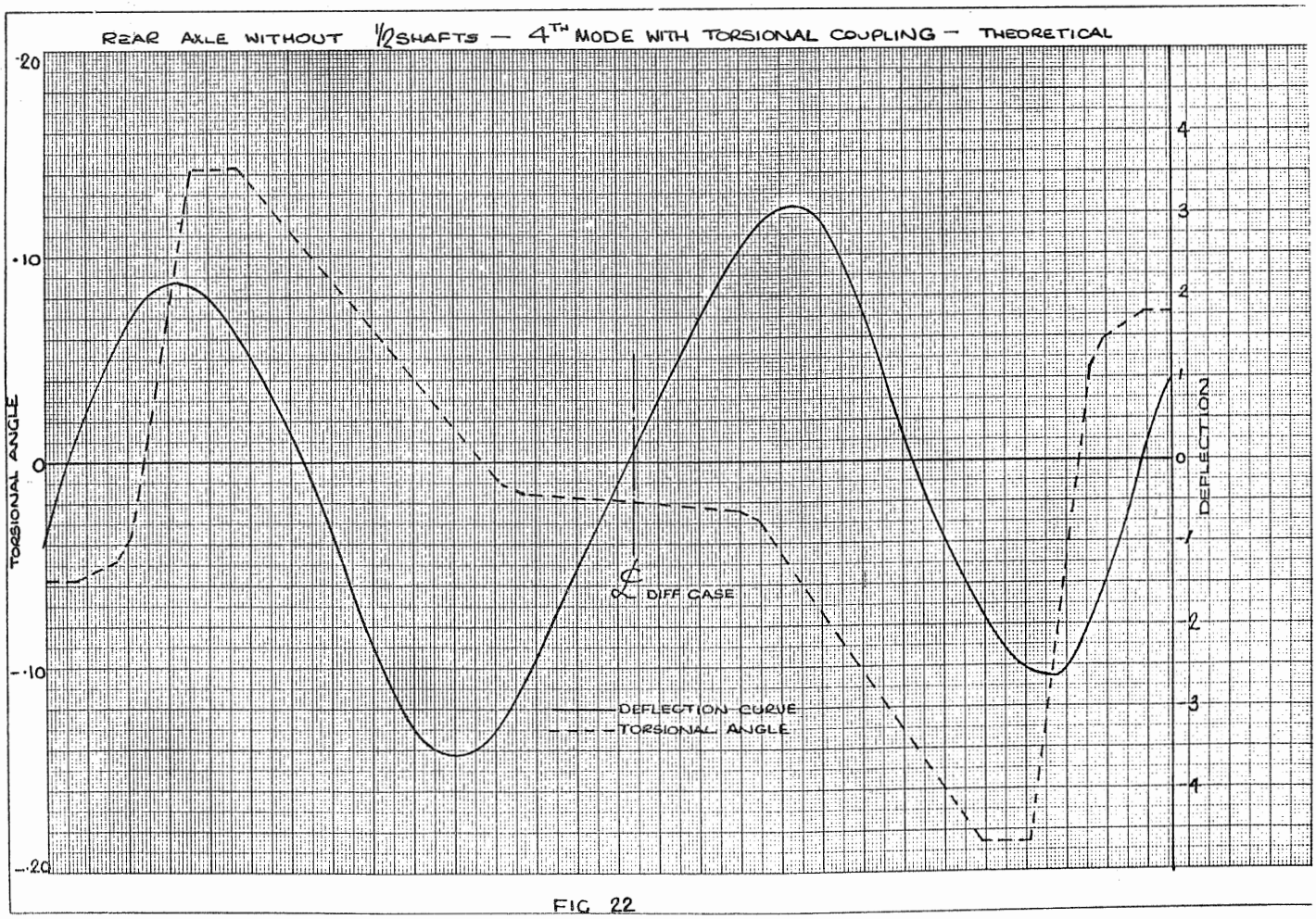
REAR AXLE WITHOUT ½ SHAFTS – 4TH MODE WITH TORSIONAL COUPLING – THEORETICAL
·20
·10
0
-·10
-·20
TORSIONAL ANGLE
DEFLECTION
4
3
2
1
0
-1
-2
-3
-4
℄ DIFF CASE
DEFLECTION CURVE
TORSIONAL ANGLE

FIG 22

REAR AXLE WITHOUT ½ SHAFTS - KENNEDY PANCU PLOT - EXPERIMENTAL

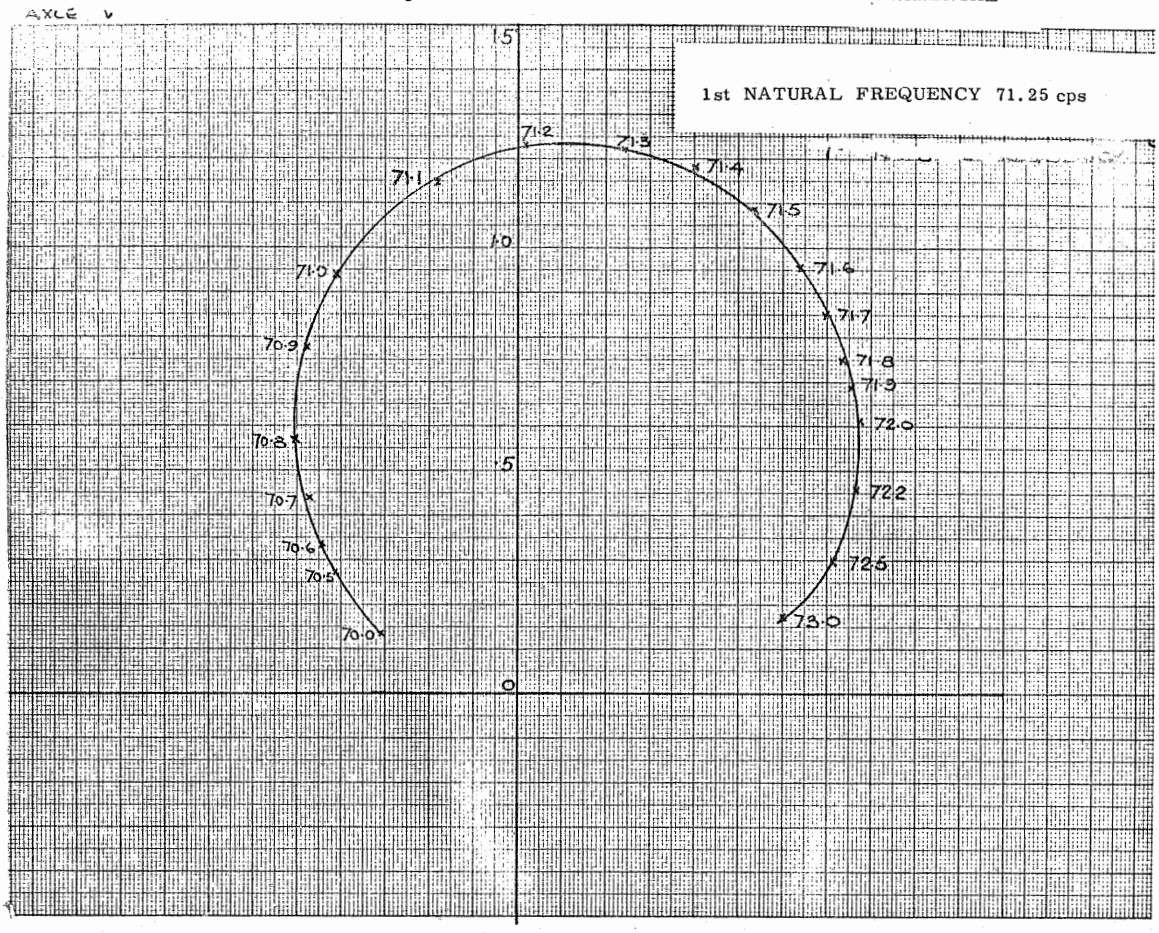

FIG 23

REAR AXLE WITHOUT ½ SHAFTS - KENNEDY PANCU PLOT - EXPERIMENTAL

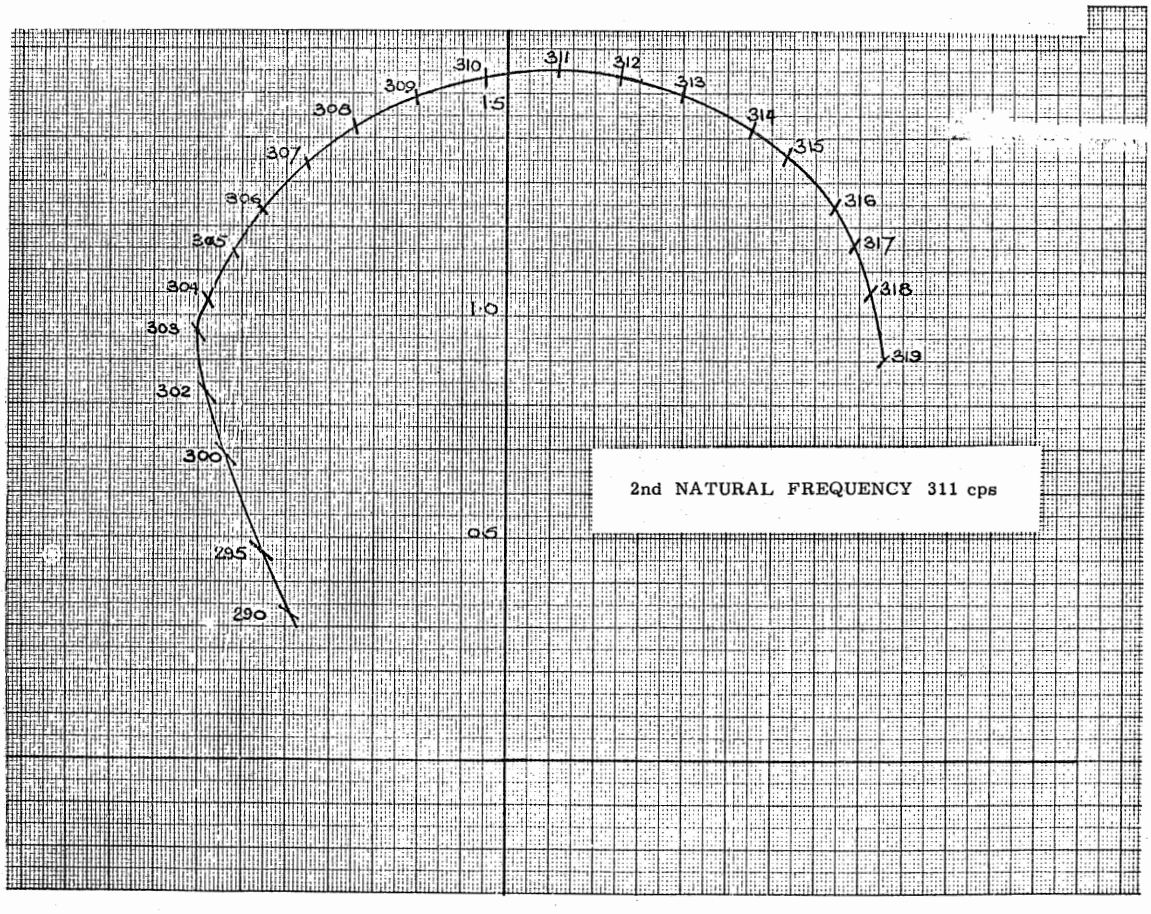

FIG 24

REAR AXLE WITHOUT $\frac{1}{2}$ SHAFTS - KENNEDY PANCU PLOT - EXPERIMENTAL

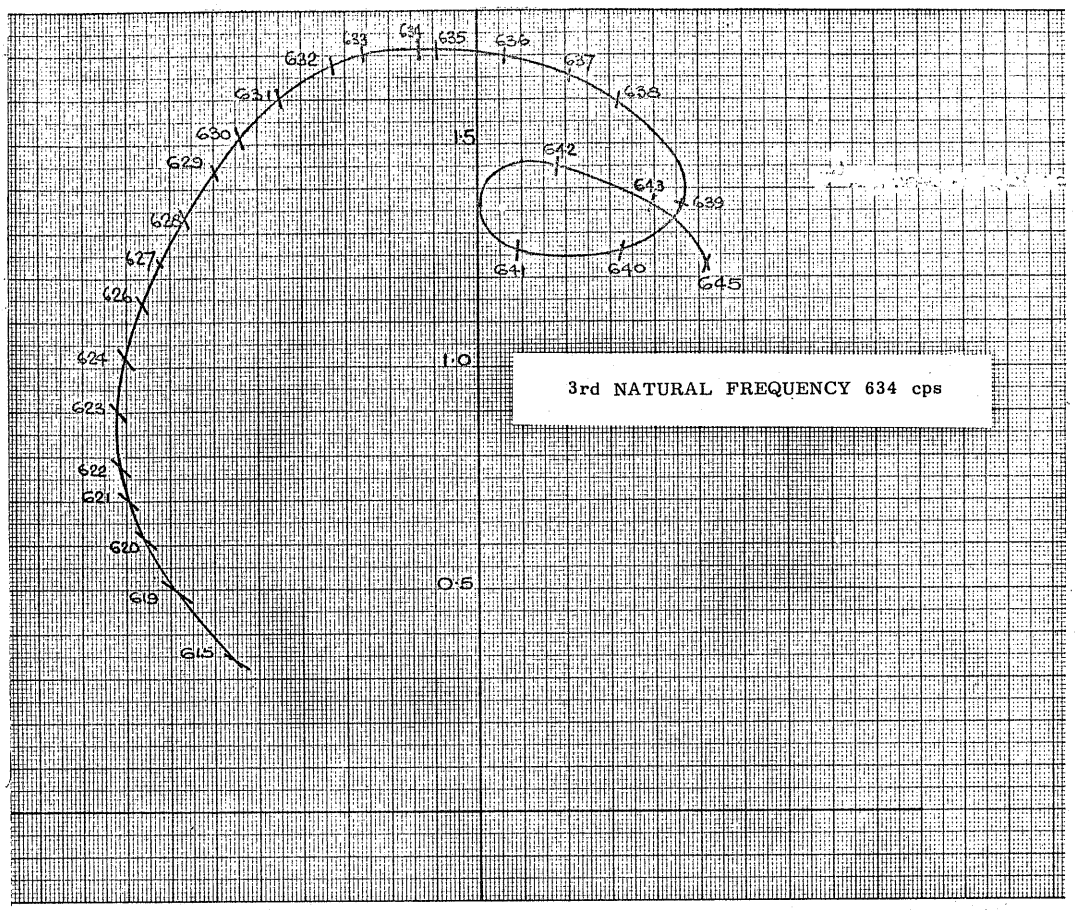

FIG 25

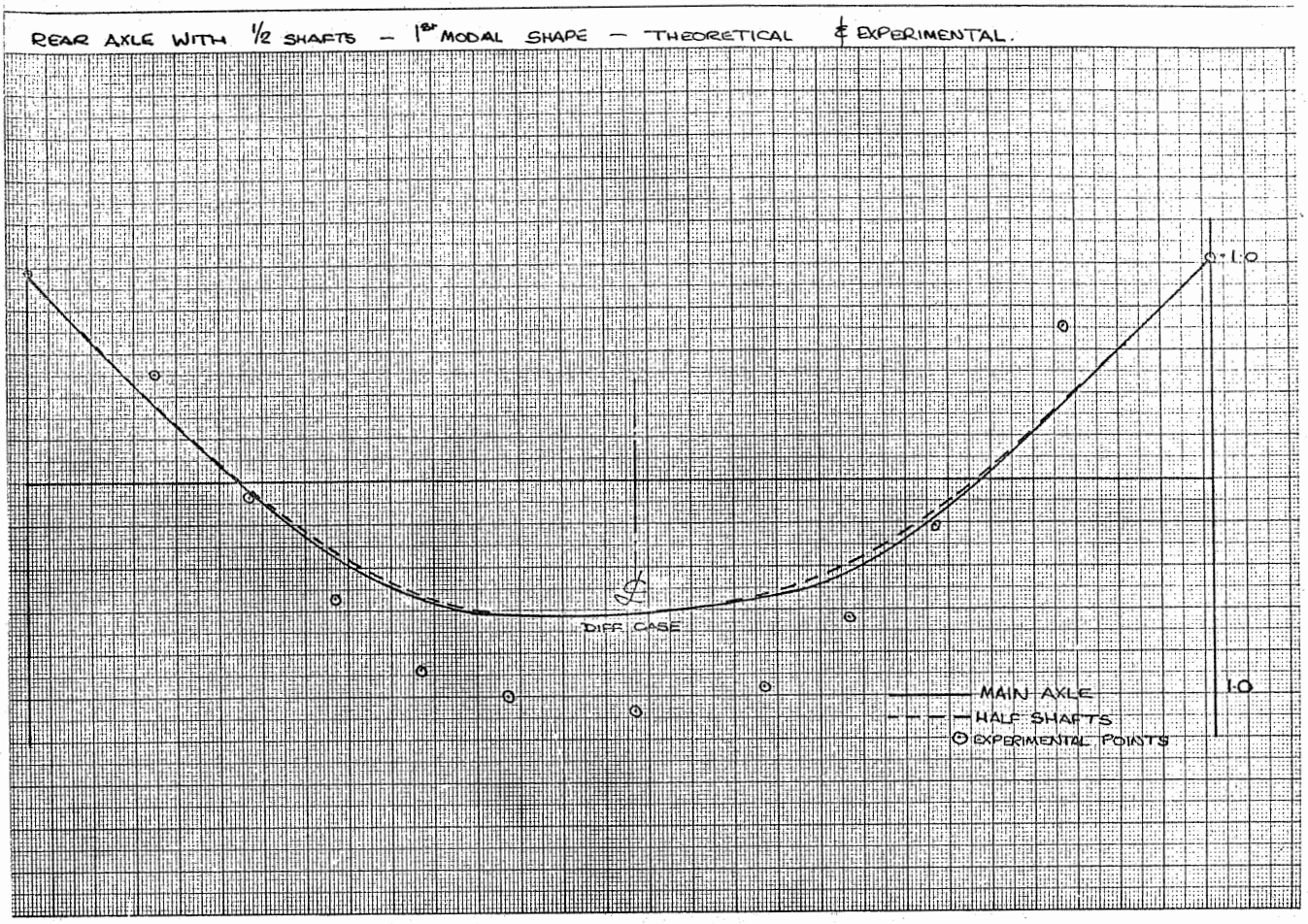
REAR AXLE WITH 1/2 SHAFTS – 1st MODAL SHAPE – THEORETICAL & EXPERIMENTAL.
1·0
DIFF. CASE
1·0
MAIN AXLE
HALF SHAFTS
EXPERIMENTAL POINTS

FIG 26

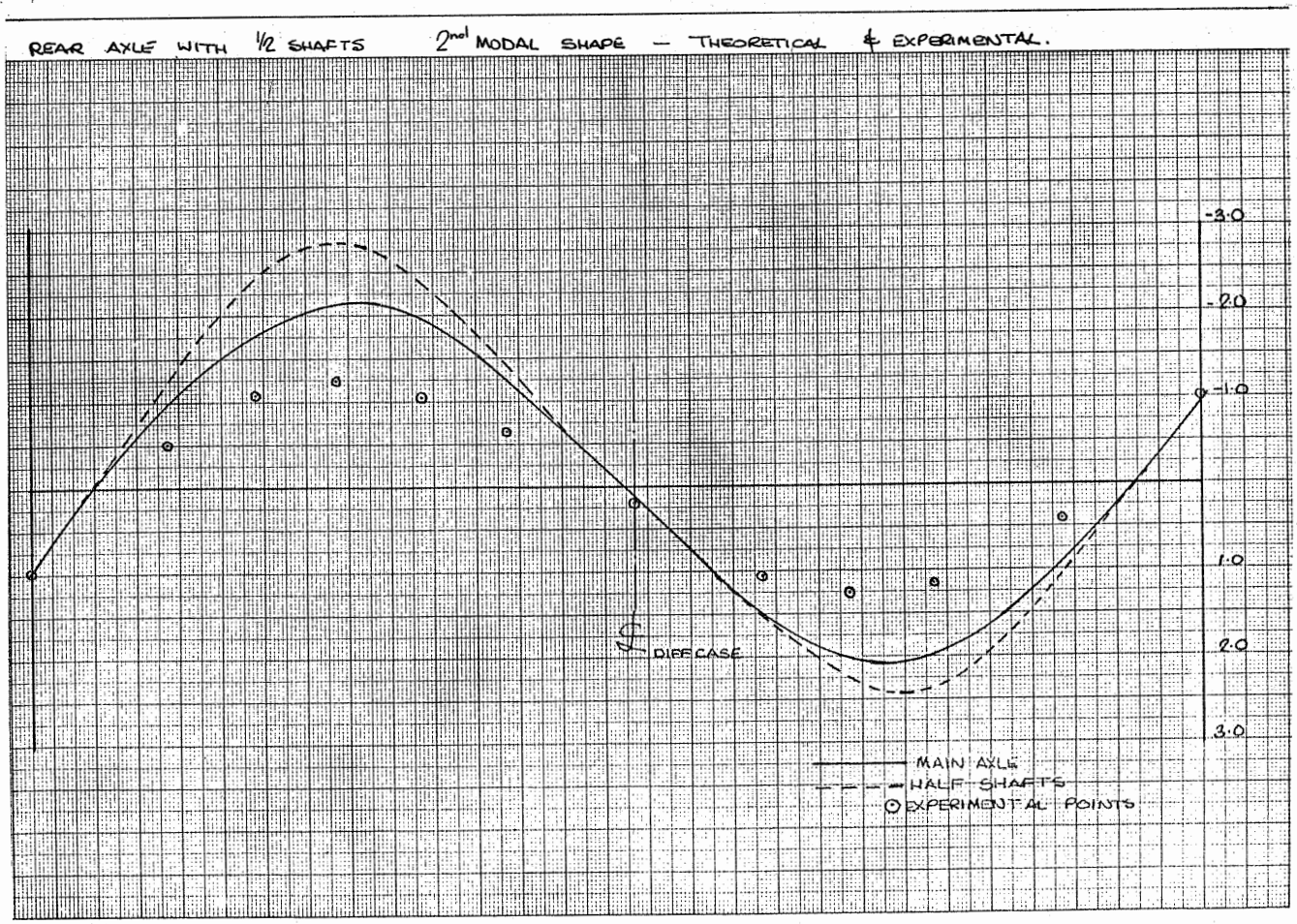
REAR AXLE WITH 1/2 SHAFTS 2nd MODAL SHAPE – THEORETICAL & EXPERIMENTAL.
3·0
2·0
1·0
1·0
2·0
3·0
DIFF CASE
MAIN AXLE
HALF SHAFTS
EXPERIMENTAL POINTS

FIG 27

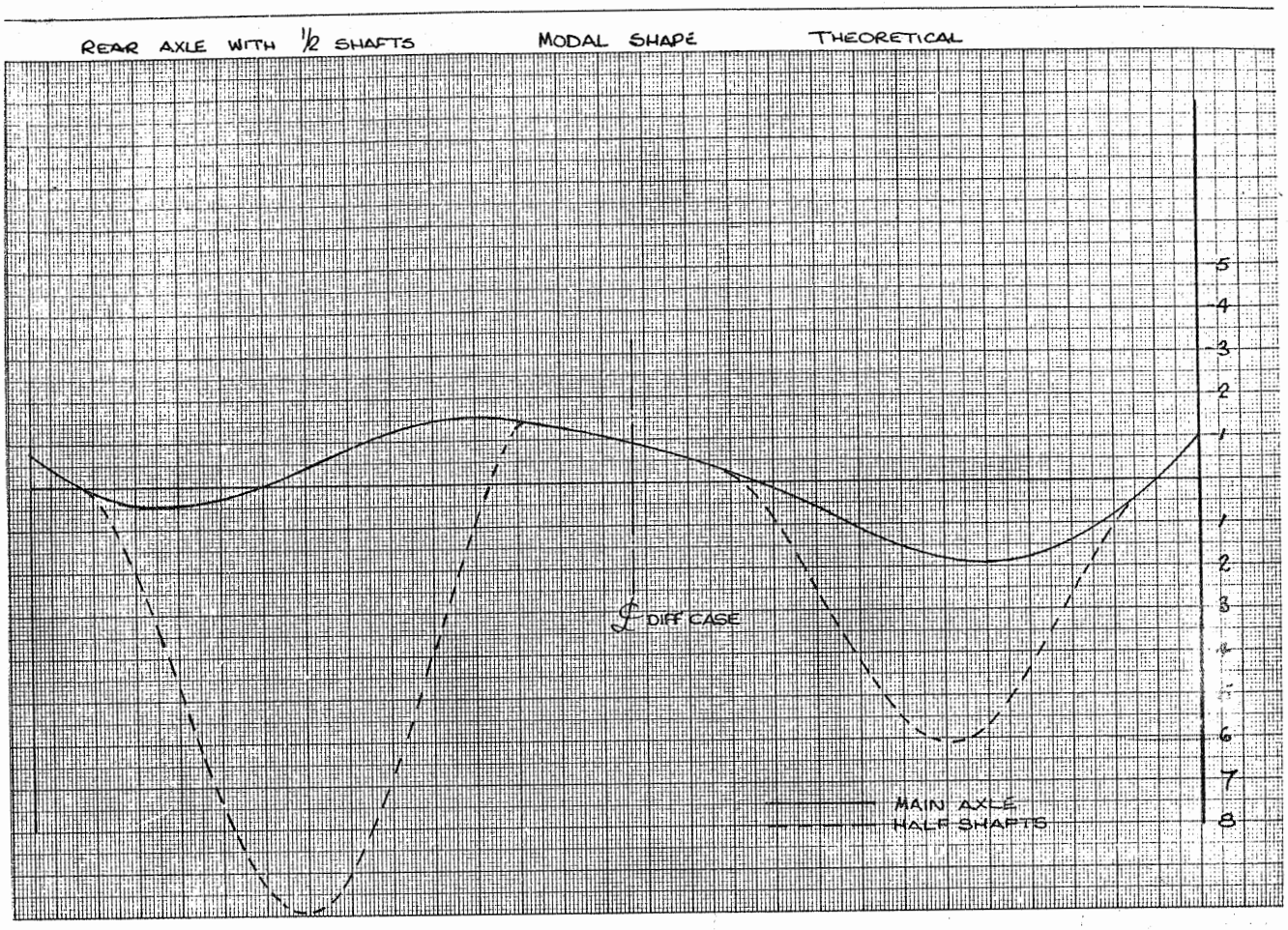
REAR AXLE WITH ½ SHAFTS
MODAL SHAPE
THEORETICAL
℄ DIFF CASE
MAIN AXLE
HALF SHAFTS

FIG 28

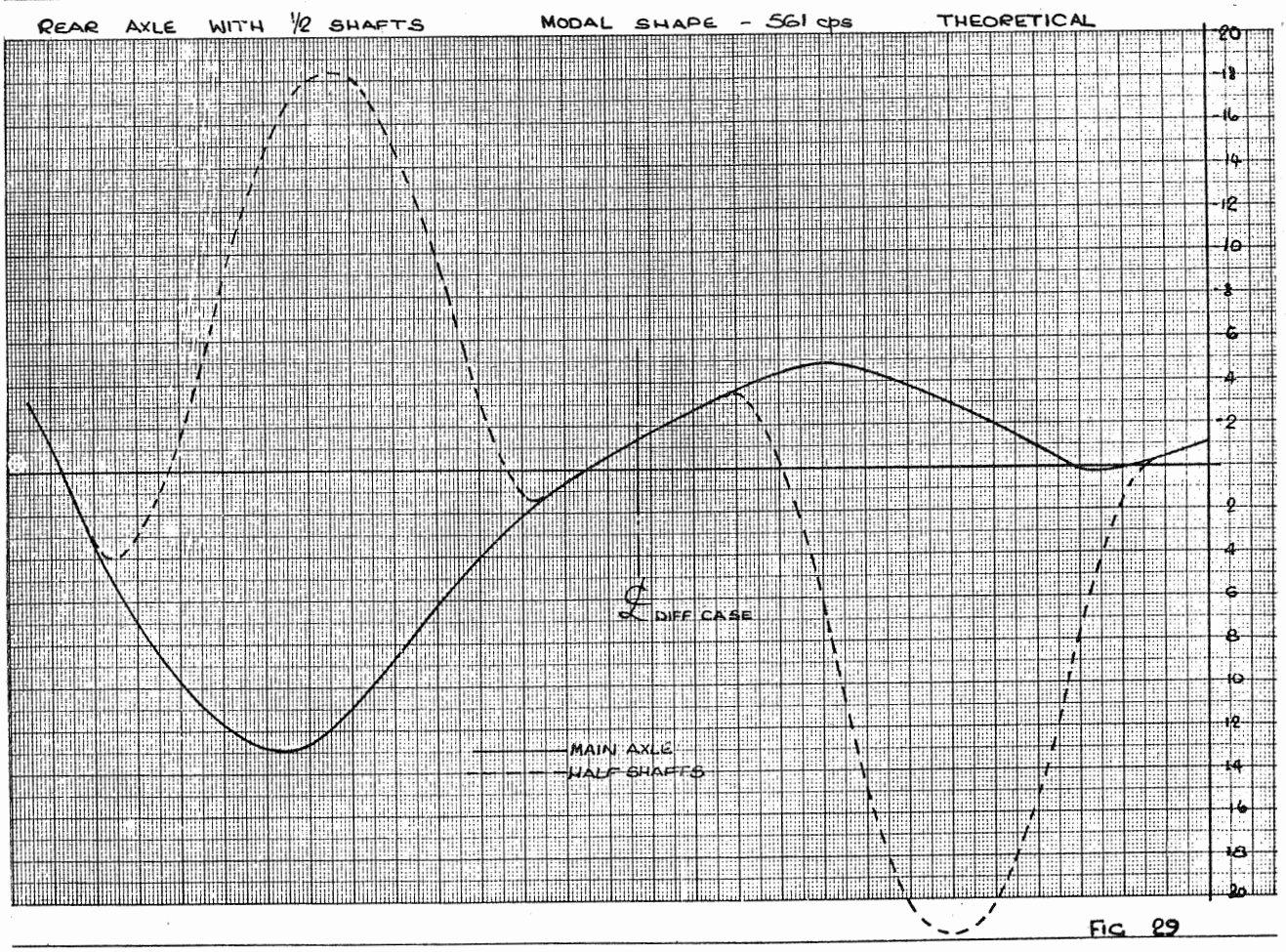
REAR AXLE WITH ½ SHAFTS
MODAL SHAPE - 561 cps
THEORETICAL
℄ DIFF CASE
MAIN AXLE
HALF SHAFTS

FIG 29

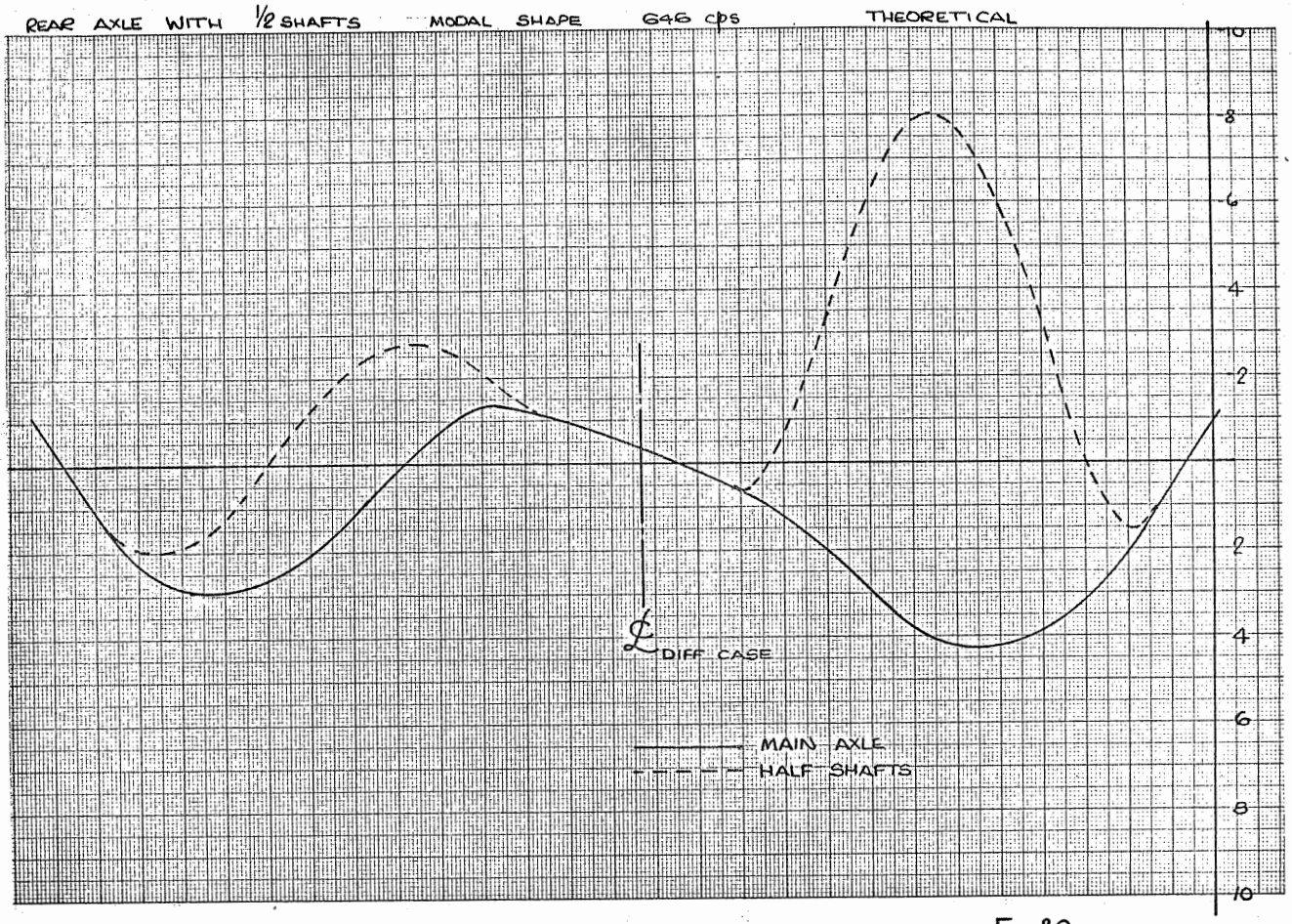
REAR AXLE WITH 1/2 SHAFTS MODAL SHAPE 646 cps THEORETICAL
10
8
6
4
2
2
4
6
8
10
℄ DIFF CASE
MAIN AXLE
HALF SHAFTS

FIG 30

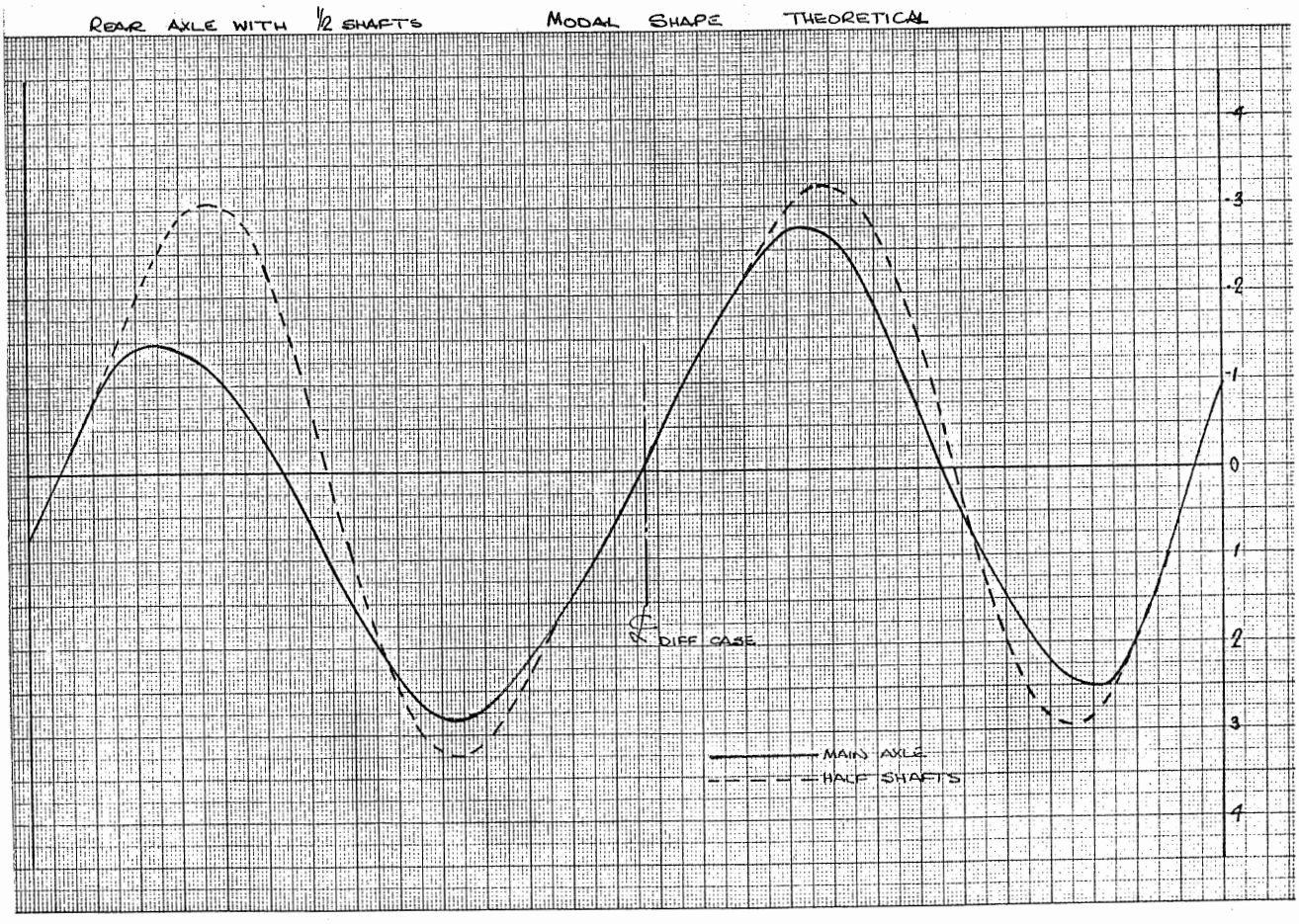
REAR AXLE WITH 1/2 SHAFTS MODAL SHAPE THEORETICAL
4
3
2
1
0
1
2
3
4
℄ DIFF CASE
MAIN AXLE
HALF SHAFTS

FIG 31

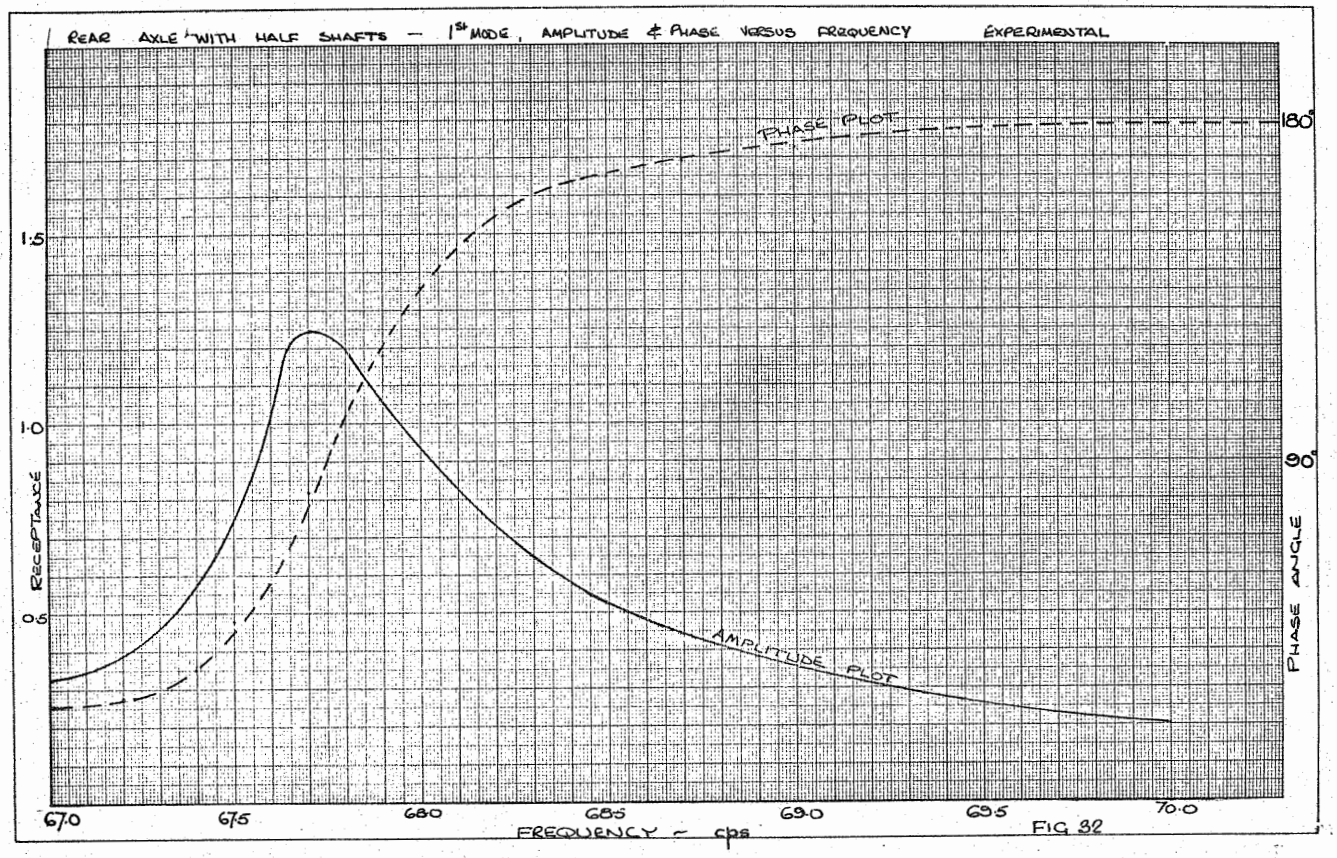
REAR AXLE WITH HALF SHAFTS — 1st MODE, AMPLITUDE & PHASE VERSUS FREQUENCY EXPERIMENTAL
PHASE PLOT
AMPLITUDE PLOT
180°
90°
1·5
1·0
0·5
RECEPTANCE
PHASE ANGLE
67·0
67·5
68·0
68·5
69·0
69·5
70·0
FREQUENCY — cps

FIG 32

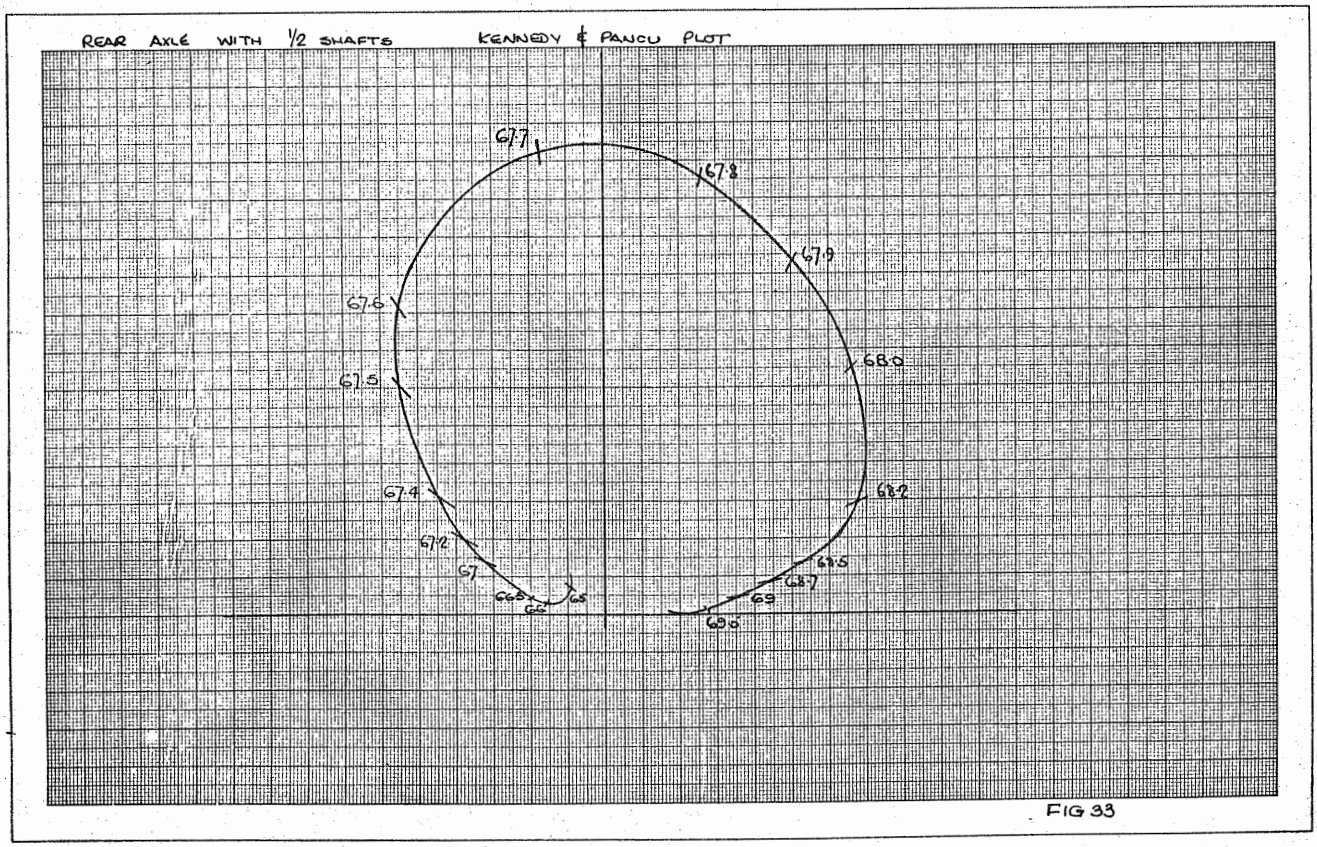
REAR AXLE WITH 1/2 SHAFTS KENNEDY & PANCU PLOT
67·7
67·8
67·9
68·0
68·2
68·5
68·7
69
68·6
67·4
67·2
67
66·8
66
65
67·5
67·6

FIG 33

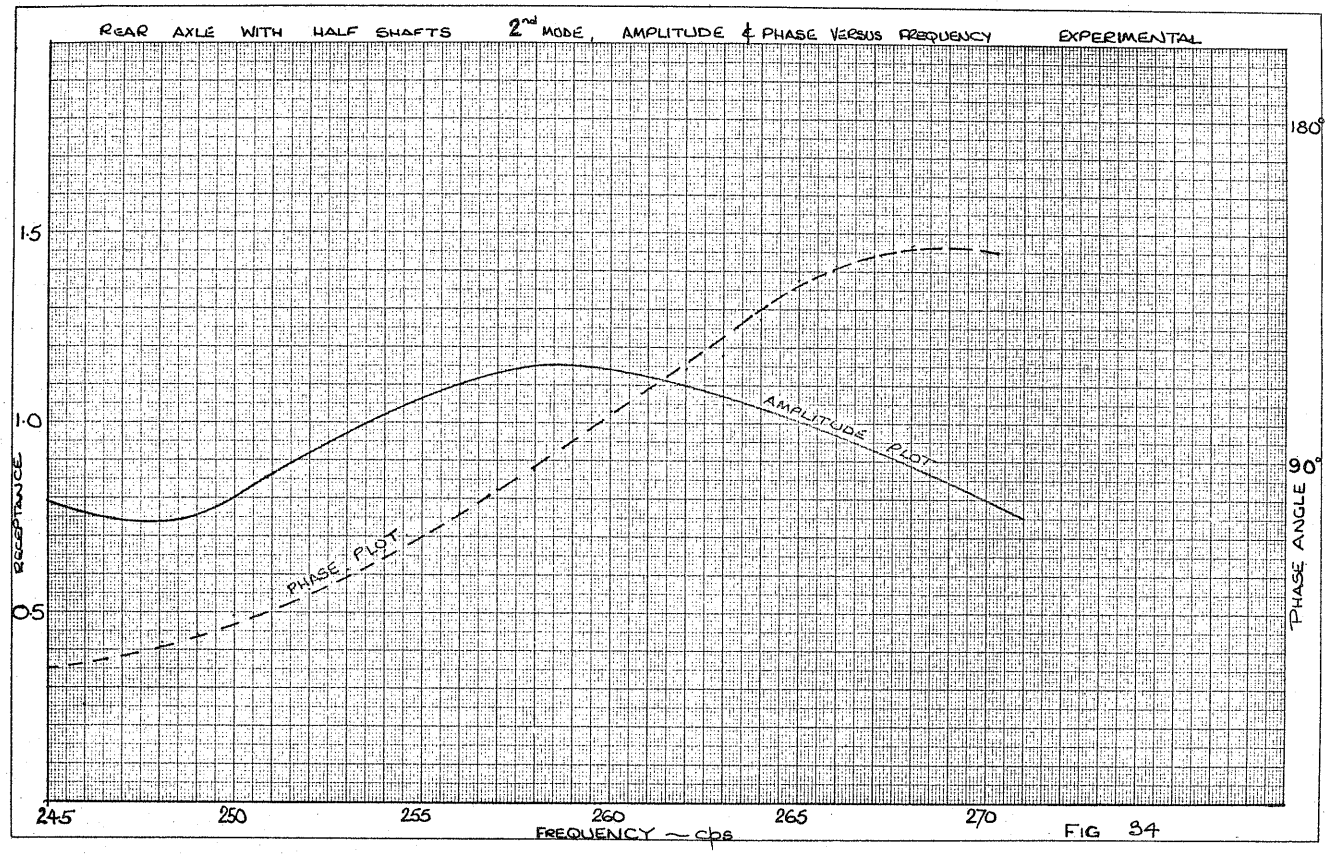
REAR AXLE WITH HALF SHAFTS 2nd MODE, AMPLITUDE & PHASE VERSUS FREQUENCY EXPERIMENTAL
RECEPTANCE
1·5
1·0
0·5
180°
90°
PHASE ANGLE
AMPLITUDE PLOT
PHASE PLOT
245
250
255
260
265
270
FREQUENCY ~ cps

FIG 34

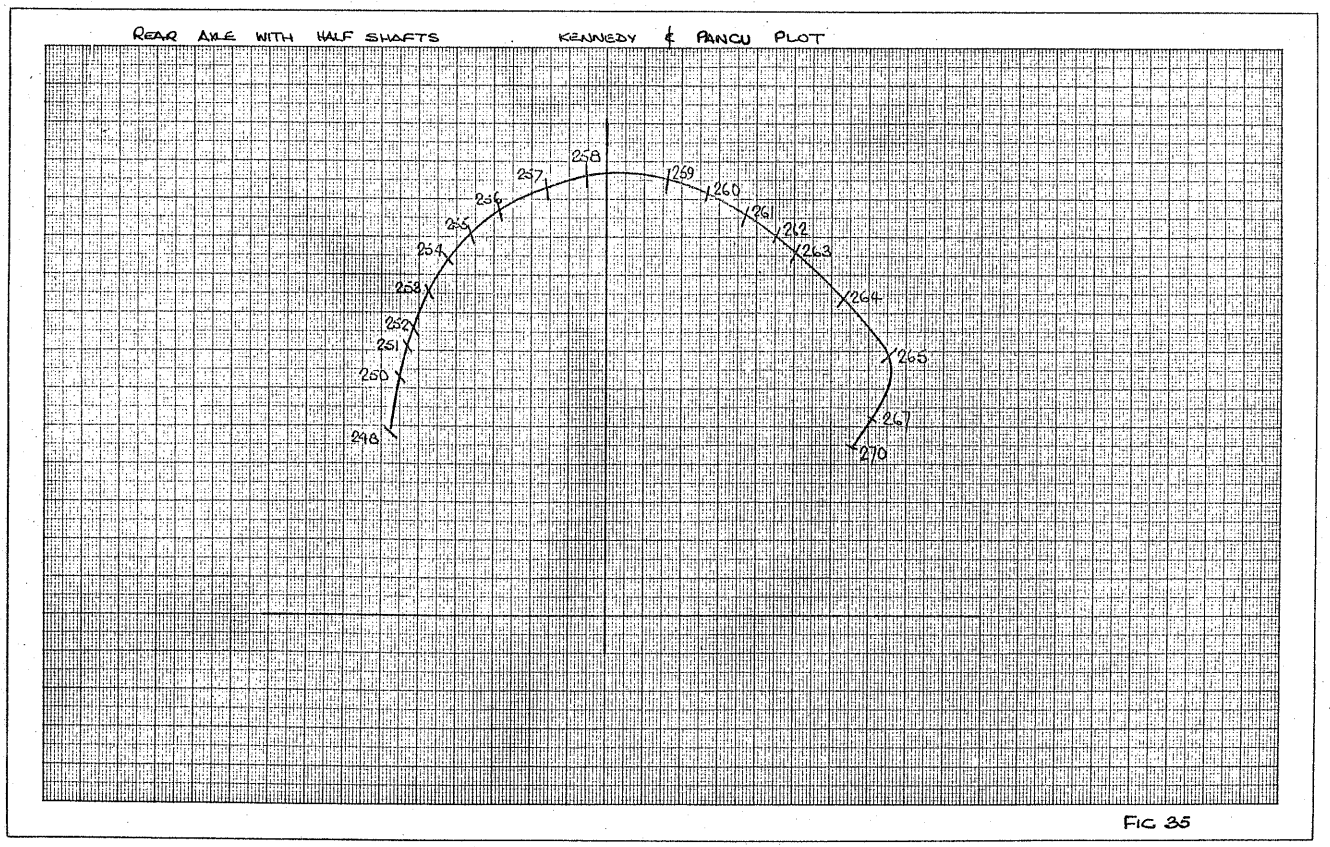
REAR AXLE WITH HALF SHAFTS KENNEDY & PANCU PLOT
248
249
250
251
252
253
254
255
256
257
258
259
260
261
262
263
264
265
266
270

FIG 35